

# The utility of methane clumped isotopes to constrain the origins of methane in natural gas accumulations

DANIEL A. STOLPER<sup>1\*</sup>, MICHAEL LAWSON<sup>2</sup>, MICHAEL J. FORMOLO<sup>2</sup>, CARA L. DAVIS<sup>2</sup>, PETER M. J. DOUGLAS<sup>3</sup> & JOHN M. EILER<sup>4</sup>

<sup>1</sup> Department of Earth and Planetary Science, University of California, Berkeley, CA 94720, USA <sup>2</sup> ExxonMobil Upstream Research Company, Spring, TX 77389, USA <sup>3</sup> Department of Earth and Planetary Sciences, McGill University, Montreal, Quebec H3A 0E8, Canada <sup>4</sup> Division of Geological and Planetary Sciences, California Institute of Technology, Pasadena, CA 91125, USA

\*Correspondence: dstolper@berkeley.edu

## Abstract

Methane clumped-isotope compositions provide a new approach to understanding the formational conditions of methane from both biogenic and thermogenic sources. Under some conditions, these compositions can be used to reconstruct the formational temperatures of the gas, and this capability can be applied to common subsets of both biogenic and thermogenic systems. Additionally, there are examples in which clumped-isotope compositions do not reflect gas-formation temperatures but instead mixing effects and kinetic phenomena; such kinetic effects also occur in common and recognizable subtypes of biogenic and thermogenic gases. Here we review the use of methane clumped-isotope measurements for understanding the origin of methane in the subsurface. We review methane clumped-isotope measurements from numerous biogenic and thermogenic natural gas reservoirs. We then place these measurements in the context of common frameworks for identifying the formational conditions of methane including the use of methane  $\delta^{13}\text{C}$  and  $\delta\text{D}$  values and  $\text{C}_1/\text{C}_{2-3}$  ratios. Finally, we propose a framework for how methane clumped isotopes can be used to identify the origin of methane accumulations.

## Introduction

Methane is an important greenhouse gas, reactant and product of microbial metabolisms, and energy resource. In general, it is the most abundant alkane in any natural gas accumulation (e.g. Mango *et al.* 1994; Hunt 1996). Methane in natural gas accumulations generally has one of two origins. First, methane can be generated by the thermally induced breakdown (also termed pyrolysis, or 'cracking') of larger hydrocarbon molecules from solid (e.g. kerogen), liquid or gaseous hydrocarbons (e.g. Tissot & Welte 1978; Hunt 1996; Seewald 2003). This methane is classified here as 'thermogenic.' Second, methane can be produced by microorganisms known as methanogens. Methanogens make methane via either the net reaction of  $\text{CO}_2$  with  $\text{H}_2$  (hydrogenotrophic methanogenesis) or the cleavage and reduction of a methyl group from larger organic molecules like acetate or

methanol (e.g. Claypool & Kaplan 1974; Rice & Claypool 1981; Thauer 1998). Methane produced by these organisms is termed 'biogenic' or microbial methane. Additionally, methane can be formed 'abiotically' through, for example, the hydrogenation of CO<sub>2</sub> in the absence of life. Such abiotic methane is not known to contribute substantial quantities of gas to economically significant hydrocarbon accumulations (e.g. Etiope & Sherwood Lollar 2013).

Establishing the origin of methane (i.e. biogenic v. thermogenic), whether for economic, biogeochemical, or environmental reasons, is generally one of the first steps in the study of hydrocarbon systems (Bernard *et al.* 1976; Schoell 1980, 1983; Whiticar *et al.* 1986; Whiticar 1999; Vinson *et al.* 2017). For example, in the study of greenhouse gas emissions, the origin of methane to the atmosphere from a given environment or setting is needed to develop emission reduction strategies (e.g. Miller *et al.* 2013). Alternatively, during petroleum exploration, the origin of methane can provide information on potential source-rock locations (if thermogenic) and the possibility of other accumulations in the area (e.g. Magoon & Dow 1994). A variety of approaches are used to identify the origin and history of hydrocarbon gases including molecular and isotopic measurements. The complexity of these approaches ranges from qualitative fingerprinting (e.g. Bernard *et al.* 1976; Schoell 1980, 1983; Whiticar *et al.* 1986) to sophisticated, quantum-mechanically grounded models of gas generation (e.g. Tang *et al.* 2000; Ni *et al.* 2011). This information is integrated with thermal histories provided by basin modelling, the stratigraphic and sedimentological evidence for the environment of deposition, and the structural analysis of trap and seal formation to understand the history of the petroleum system. This integrated approach is required to predict the potential distribution of hydrocarbons both spatially and temporally.

Here, we review the utility of measuring methane isotopologues with multiple heavy isotopes (e.g. both <sup>13</sup>C and deuterium (D)), which are colloquially referred to as 'clumped' isotopologues (Eiler 2007), to study the origin of methane. We review the conditions under which methane clumped-isotope measurements yield quantitative and usefully precise measures of a gas's formation temperature. We additionally address examples where the clumped-isotopic composition does not yield a meaningful formation temperature but instead relates to formational mechanisms. We specifically highlight the constraints methane clumped isotopes can provide on the origin of both biogenic and thermogenic natural gas deposits. This review places methane clumped isotopes into the broader framework of tools used to study hydrocarbon systems including standard molecular and isotopic techniques. Douglas *et al.* (2017) provides a broader review for methane clumped-isotope measurements beyond hydrocarbon systems.

Conventional molecular and isotopic techniques used to study the origins of hydrocarbon gases

Here we review two frameworks commonly used to identify the origin of methane in a given environment. Later in the review we place clumped-isotope measurements of methane into the context of these frameworks. We do not attempt to review all classification schemes here (e.g. Schoell 1983; Chung *et al.* 1988; Ballentine & O'Nions 1994; Prinzhofer & Huc 1995; Lorant *et al.* 1998).

One composition space used to map out the origin of methane in natural gas deposits is the 'Whiticar' plot (Fig. 1a; Whiticar *et al.* 1986; Whiticar 1999). It is empirical in nature and involves the comparison of an unknown sample with a two-dimensional isotopic map that delineates gas origins (biogenic, thermogenic or a mixture of the two) using the  $\delta D$  and  $\delta^{13}C$  values of methane. This map is based on isotopic measurements of methane with independently known origins. The composition space defined by the Whiticar plot separates biogenic from thermogenic methane as follows: biogenic methane always has, at a given  $\delta D$  value, a lower  $\delta^{13}C$  value than thermogenic methane. Depending on the  $\delta D$  value, the  $\delta^{13}C$  cut-off for defining biogenic v. thermogenic gas can vary from  $-45$  to  $-60\text{‰}$ . Additionally, although thermogenic and biogenic methane overlap extensively in  $\delta D$  values (overlapping from c.  $-150$  to  $-275\text{‰}$ ), biogenic methane can have significantly lower  $\delta D$  values (below  $-400\text{‰}$ ) while thermogenic gases can have  $\delta D$  values as high as  $-100\text{‰}$ . Finally, the category of 'mixed/overlap' in the Whiticar plot indicates gases that are either mixtures of biogenic and thermogenic gas, or a composition where thermogenic and biogenic gases cannot be distinguished.

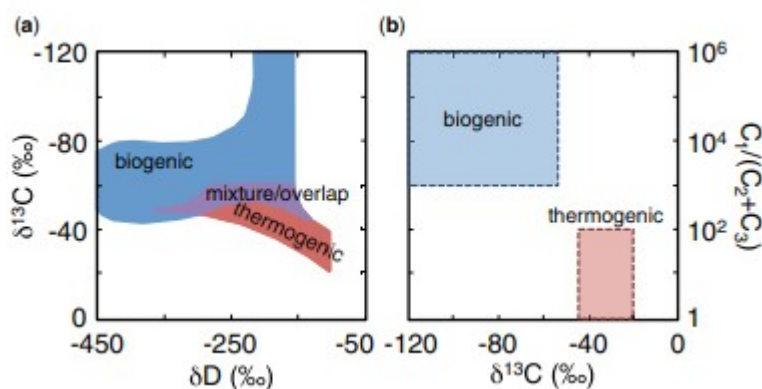


Fig. 1.

Common composition spaces used to identify the origin of methane from environmental samples. (a) The 'Whiticar' plot (Whiticar *et al.* 1986; Whiticar 1999) uses the  $\delta D$  and  $\delta^{13}C$  values of methane to distinguish biogenic and thermogenic gases from one another. (b) The 'Bernard' plot (Bernard *et al.* 1976) uses the  $C_1/C_{2-3}$  ratio v. the  $\delta^{13}C$  value of methane to distinguish thermogenic from biogenic gas. Many versions of the Bernard plot exist, with different boundaries (e.g. Vinson *et al.* 2017). The boundaries given here are those given in Martini *et al.* (1996). Additionally, pathways of diffusion, mixing and methane oxidation are sometimes plotted in these spaces (e.g. Whiticar 1999; Etiope & Sherwood Lollar 2013; Vinson *et al.* 2017).

Another composition space used to establish the origin of a sample of methane is the 'Bernard' plot (Fig. 1b; Bernard *et al.* 1976). The Bernard plot

differentiates thermogenic from biogenic gases using methane  $\delta^{13}\text{C}$  values and  $\text{C}_1/\text{C}_{2-3}$  ratios.  $\text{C}_1/\text{C}_{2-3}$  ratios quantify the relative abundance of methane ( $\text{C}_1$ ) to the sum of ethane ( $\text{C}_2$ ) and propane ( $\text{C}_3$ ).  $\text{C}_1/\text{C}_{2-3}$  ratios are used to distinguish biogenic from thermogenic gases because, in biogenic systems, methane is generally the main hydrocarbon generated (generally >99%). Thermogenic gases, in contrast can contain significant quantities (up to tens of per cent) of alkanes larger than methane ( $\text{C}_2+$  alkanes). In the Bernard plot, biogenic gases are defined to have  $\text{C}_1/\text{C}_{2-3}$  values greater than 1000 while thermogenic gases have  $\text{C}_1/\text{C}_{2-3}$  values less than 100. Higher  $\text{C}_1/\text{C}_{2-3}$  values for thermogenic gases may be achieved via compositional fractionations induced during migration (Bernard *et al.* 1977).

In addition to these composition spaces, it is generally assumed that both the  $\delta^{13}\text{C}$  and  $\delta\text{D}$  values of methane and  $\text{C}_1/\text{C}_{2-3}$  ratios increase over the course of petroleum generation. The extent of hydrocarbon generation generally increases with increasing burial temperature (and time spent at a given temperature) of the source rock. Consequently, the position of a thermogenic gas in the Bernard and Whiticar plots within the nominally thermogenic field is indicative of the 'thermal maturity' of the gas's source rock at the time of the gas's generation (Stahl & Carey 1975; Schoell 1980, 1983; Chung *et al.* 1988; Rooney *et al.* 1995; Hunt 1996; Tang *et al.* 2000; Ni *et al.* 2011).

The Whiticar and Bernard plots are useful for identifying the origin of methane in the environment. However, the criteria used on these plots to delineate biogenic from thermogenic methane are not always definitive. Specifically, in these plots, a gas with a  $\text{C}_1/\text{C}_{2-3}$  ratio greater than 1000 and  $\delta^{13}\text{C}$  value less than  $-60\text{‰}$  will always be classified as biogenic and a gas with a  $\text{C}_1/\text{C}_{2-3}$  ratio less than 100 and  $\delta^{13}\text{C}$  greater than  $-50\text{‰}$  will always be classified as thermogenic. However, some suspected biogenic methane occurrences have methane  $\delta^{13}\text{C}$  values as high as  $-45\text{‰}$  (Martini *et al.* 1996). Additionally,  $\text{C}_1/\text{C}_{2-3}$  values in modern marine sediments can be as low as 2 under conditions where ethane and propane are also biogenic in origin (Hinrichs *et al.* 2006). Moreover, the model of Tang *et al.* (2000) predicts that thermogenic methane generated at temperatures less than  $180^\circ\text{C}$  in nature can have  $\delta^{13}\text{C}$  values between  $-60$  to  $-70\text{‰}$ . Finally, thermogenic gases trapped in 'unconventional' shale-gas deposits ('shale gases') can have  $\text{C}_1/\text{C}_{2-3}$  values greater than 1000 (e.g. Stolper *et al.* 2014a). These counter-examples illustrate that, while empirical classification schemes such as the Whiticar and Bernard plots are useful for interpreting the origins of natural gas deposits, they are not always clear-cut. Such counter-examples have led to alternative delineations of methane sources in  $\delta\text{D}$  v.  $\delta^{13}\text{C}$  and  $\text{C}_1/\text{C}_{2-3}$  v.  $\delta^{13}\text{C}$  plots (e.g. Etiope & Sherwood Lollar 2013; Vinson *et al.* 2017). This demonstrates that such spaces serve as useful starting points for the identification of methane sources, but they are not always definitive.

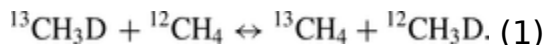
One physical variable often associated with the origin of a gas is its formation temperature. Biogenic gases are generally thought to form in

nature from c. 0°C to 80°C (Wilhelms *et al.* 2001; Valentine 2011), though pure cultures of methanogens can grow in the laboratory at temperatures at least as high as 122°C (Takai *et al.* 2008). In contrast, thermogenic gases are thought to form at temperatures above c. 60°C (Tissot & Welte 1978; Quigley & Mackenzie 1988; Hunt 1996; Seewald *et al.* 1998; Seewald 2003). Furthermore, some models predict that most thermogenic gases form above 150°C (Quigley & Mackenzie 1988). Thus, measurements of methane formation temperatures could provide an additional parameter for understanding the genesis of hydrocarbon gases. Additionally, such a tool would allow for insights into the geological history of sedimentary basins by providing constraints on the minimum temperatures a given source rock (that generated methane) reached during burial. We now discuss how clumped-isotope measurements of methane, can, under some circumstances, be used to measure methane formational temperatures in a variety of hydrocarbon systems. First we briefly review the theory and measurement of methane clumped isotopes.

#### Theory and nomenclature of methane clumped-isotope measurements

Clumped isotopologues are any molecules with two or more rare (generally heavy) isotopes (Eiler & Schauble 2004; Wang *et al.* 2004; Eiler 2007). An example of a methane clumped isotopologue is  $^{13}\text{CH}_3\text{D}$ . Such isotopologues are of geological and geochemical interest because, for a population of molecules in isotopic equilibrium with one another, their abundance is controlled solely by the system's average or 'bulk' isotopic composition (constrained by its  $\delta\text{D}$  and  $\delta^{13}\text{C}$  values) and the system's temperature (e.g. Wang *et al.* 2004).

Take the following isotope-exchange reaction between various methane isotopologues:



At equilibrium, the relative abundances of the isotopologues in equation (1) are controlled by the reaction's equilibrium constant. This equilibrium constant is a monotonic function of temperature (Ma *et al.* 2008; Cao & Liu 2012; Ono *et al.* 2014; Stolper *et al.* 2014*b*; Webb & Miller III 2014; Liu & Liu 2016). Additionally, for an isotopically equilibrated system the left side of the equation, which contains the clumped isotopologue ( $^{13}\text{CH}_3\text{D}$ ), is always favoured relative to the right side at finite temperatures. This leads to a unique excess of  $^{13}\text{CH}_3\text{D}$  at a given temperature (with larger excesses at lower temperatures) compared to that expected for a random distribution of isotopes amongst all isotopologues. This random distribution is constrained by the average isotopic composition of the methane (i.e. the  $\delta\text{D}$  and  $\delta^{13}\text{C}$  values, which are measureable themselves). Consequently, if the abundance of  $^{13}\text{CH}_3\text{D}$  or other clumped isotopologues can be constrained along with the  $\delta\text{D}$  and  $\delta^{13}\text{C}$  values, an 'apparent' clumped-isotope-based methane formation temperature can be calculated. This apparent temperature will only reflect a true formation temperature if the methane formed in isotopic equilibrium

and maintained that composition up until analysis. This is a key requirement that, as we discuss below, is apparently met in some but not all cases. We note that the actual reactions that allow isotopic equilibrium to be achieved between various methane isotopologues are not restricted to reactions involving only methane (i.e. reactions like those in equation 1), but instead are probably achieved via isotope-exchange reactions with other molecules including H<sub>2</sub>O, H<sub>2</sub> or CO<sub>2</sub>. Rather, the sorts of isotope-exchange reactions as given in equation (1) provide a framework for calculating equilibrium constants for systems in isotopic equilibrium regardless of the reactions that allow that equilibrium to be achieved (Urey 1947). More thorough reviews of the theory of clumped isotopes can be found in Wang *et al.* (2004), Eiler (2007), Affek (2012) and Eiler (2013).

The abundance of clumped isotopologues is reported relative to a calculated abundance that assumes all isotopes are randomly distributed amongst all isotopologues. This distribution is referred to as random or ‘stochastic’. The clumped-isotopic composition of a sample is reported using  $\Delta$  notation (Wang *et al.* 2004) such that, for example,

$$\Delta_{13\text{CH}_3\text{D}} = \left( \frac{{}^{13}\text{CH}_3\text{D}_R}{{}^{13}\text{CH}_3\text{D}_R^*} - 1 \right) \times 1000. \quad (2)$$

Here,  ${}^{13}\text{CH}_3\text{D}_R = [{}^{13}\text{CH}_3\text{D}]/[{}^{12}\text{CH}_4]$  and the \* indicates the ratio that would be observed if all isotopes are randomly distributed amongst all isotopologues. As discussed in Wang *et al.* (2004) and specifically for methane in Stolper *et al.* (2014b),  $\Delta$  values are related to the equilibrium constants of isotope-exchange reactions. Specifically,  $\Delta_{13\text{CH}_3\text{D}}$  is related to the equilibrium constant for reaction (1),  $K_{13\text{CH}_3\text{D}}$ , as follows:

$$\Delta_{13\text{CH}_3\text{D}} \cong -1000 \times \ln(K_{13\text{CH}_3\text{D}}). \quad (3)$$

The approximate sign is included due to the potential second-order effects of non-random proportions of  ${}^{13}\text{CH}_4$  and  ${}^{12}\text{CH}_3\text{D}$ . This is unimportant for samples with  $\delta\text{D}$  and  $\delta^{13}\text{C}$  values typical of those found in natural materials (see discussion in Stolper *et al.* (2014b)). Thus, a  $\Delta_{13\text{CH}_3\text{D}}$  value is directly related to the equilibrium constant for the clumped-isotope reaction in equation (1) and can be used to calculate a gas-formation temperature.

For reasons related to how the majority of methane clumped-isotope measurements presented here were made (discussed in the next section), this review primarily uses a subtly different  $\Delta$  notation. Specifically, the majority of methane clumped-isotope abundances reported in this review combine the abundances of both of methane's mass-18 clumped isotopologues,  ${}^{13}\text{CH}_3\text{D}$  and  ${}^{12}\text{CH}_2\text{D}_2$ . We report their combined abundances relative to  ${}^{12}\text{CH}_4$  v. the random isotopic distribution using  $\Delta_{18}$  notation such that:

$$\Delta_{18} = \left( \frac{{}^{18}\text{R}}{{}^{18}\text{R}^*} - 1 \right) \times 1000. \quad (4)$$

Here,  $^{18}R = ([^{13}\text{CH}_3\text{D}] + [^{12}\text{CH}_2\text{D}_2])/[^{12}\text{CH}_4]$ .

As 98% of mass-18 methane is  $^{13}\text{CH}_3\text{D}$ , inclusion of  $^{12}\text{CH}_2\text{D}_2$  is unimportant for most applications within the error of the measurement (though the difference could be important in certain cases where significant kinetic isotope effects are expressed) – this is discussed in detail in Stolper *et al.* (2014*b*). We provide a calculation of the dependence of  $\Delta_{18}$  on temperature from 0 to 300°C in Figure 2. This range delineates the field of values where biogenic and thermogenic gases would likely be found if the methane formed in isotopic equilibrium.

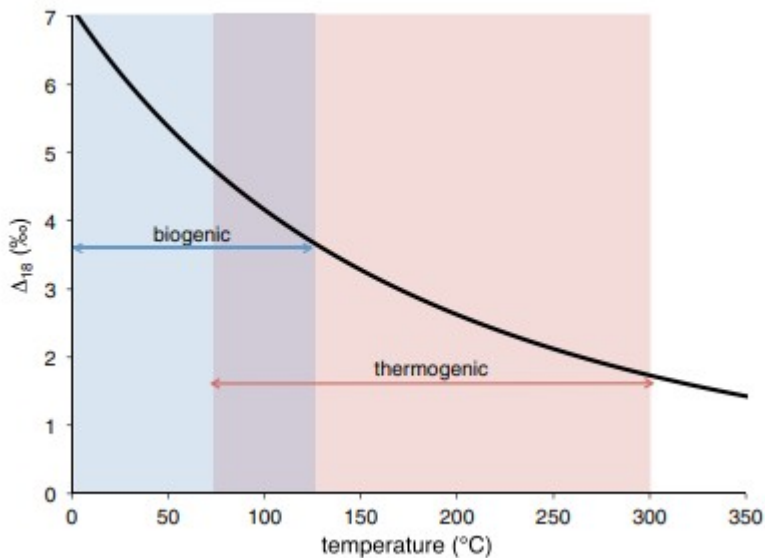


Fig. 2.

Equilibrium dependence of  $\Delta_{18}$  on temperature. Modified from Stolper *et al.* (2014*b*). Expected ranges are given for biogenic and thermogenic gases formed in clumped-isotopic equilibrium. The overall thermogenic range is derived from the start of the oil window of *c.* 60°C (Hunt 1996) through *c.* 300°C; 300°C is the approximate modelled maximum temperature of methane generation (e.g. Behar *et al.* 1992; Tsuzuki *et al.* 1999; Vandenbroucke *et al.* 1999; Tang *et al.* 2000; Dominé *et al.* 2002; Burruss & Laughrey 2010), though the maximum temperature of thermogenic gas generation is poorly constrained (Seewald 2003). The maximum temperature of biogenic methane generation (122°C) is taken from the experiments of Takai *et al.* (2008).

We note that before the first clumped-isotope measurements of methane were made it was not clear whether  $\Delta_{18}$  values would reflect equilibrium-based formation temperatures or kinetic processes reflecting methane generation, migration or extraction. Formation temperatures can only be meaningfully calculated from clumped-isotope abundances if the methane formed in internal isotopic equilibrium. Most previous interpretations of  $\delta^{13}\text{C}$  and  $\delta\text{D}$  values of both thermogenic and biogenic methane invoked kinetic isotope effects to describe the observed isotopic compositions (Whiticar *et al.* 1986; Espitalie *et al.* 1988; Clayton 1991; Hunt 1996; Whiticar 1999; Tang *et al.* 2000; Xiao 2001; Seewald 2003; Valentine *et al.* 2004; Ni *et al.* 2011). Therefore the capacity to use clumped-isotope abundances to measure meaningful methane formation temperatures was not obvious prior to the

study of natural gases and those generated in the lab to mimic gas-formational conditions.

### Measurements of methane clumped isotopologues

Multiple techniques currently exist for accurate and precise (sub per mille) variations in mass-18 methane isotopologue abundances. The first such technique was described by Stolper *et al.* (2014b), who used a prototype 'high-resolution' gas-source isotope-ratio mass spectrometer (the Thermo Scientific MAT 253 Ultra) detailed in Eiler *et al.* (2013). The critical enabling feature of this mass spectrometer is its capacity to cleanly separate  $\text{H}_2^{16}\text{O}$  (18.011 amu), a ubiquitous contaminant in all mass spectrometers, from  $^{13}\text{CH}_3\text{D}$  (18.041 amu). The external precision (1 standard deviation;  $\sigma$ ) for  $\Delta_{18}$  measurements made on c. 50 micromoles of pure methane (c. 1 ml at STP) is  $\pm 0.25$  ‰. The majority (83%) of data discussed here come from measurements made on this instrument.

Following this mass spectrometric technique, Ono *et al.* (2014) described a technique for measuring abundances of  $^{13}\text{CH}_3\text{D}$  (constraining ) using infrared spectroscopy accurately and precisely. Although precision depends on the amount of gas analysed, internal precisions of  $\pm 0.1$  ‰ ( $1\sigma$ ) can be achieved using c. 450 micromoles (10 ml at STP) of pure methane. Most of the data discussed here were derived using these two techniques (96%) with the remainder from the recently commissioned Nu Instruments Panorama (see below).

More advanced mass spectrometric techniques for measuring both  $^{13}\text{CH}_3\text{D}$  and  $^{12}\text{CH}_2\text{D}_2$  abundances separately are now ready. Production-line versions of the Mat 253 Ultra (Clog *et al.* 2015; Ellam *et al.* 2015) as well as another prototype high-resolution gas-source isotope-ratio mass spectrometer (the Nu Panorama; Young *et al.* 2016) have both been shown to be capable of resolving  $^{13}\text{CH}_3\text{D}$  and  $^{12}\text{CH}_2\text{D}_2$  from each other and various ion adducts. Additionally, advances in infrared spectroscopy may also permit analysis of both of these clumped isotopologues of methane. Thus, methane clumped-isotope measurements involving separate measurements of  $^{13}\text{CH}_3\text{D}$  and  $^{12}\text{CH}_2\text{D}_2$  abundances will be one of the next forefronts of methane clumped-isotope geochemistry.

### Methane clumped-isotope measurements of thermogenic gases

Here, we review the dataset of current methane clumped-isotope measurements from both experimental simulations of hydrocarbon generation and environmental settings. We classify thermogenic gases using two criteria related to the physical and chemical conditions present in a hydrocarbon deposit. The first criterion is whether or not the gas was formed in place in the reservoir, or migrated from its formational location. Natural gas deposits in which the stratigraphic location where the gas forms and remains trapped are identical are termed 'unconventional' deposits (Curtis 2002). In most unconventional deposits, the reservoir (and source) rock is



shale and it must be hydraulically fractured in order to create permeability for gas or oil extraction. In contrast, 'conventional' reservoirs are those in which hydrocarbons formed elsewhere (the 'source rock') and became trapped during migration from their source. These are termed conventional because they have been, historically, the typical accumulations of hydrocarbon liquids and gases.

These designations are significant for our purposes. Conventional reservoirs can accumulate gases from a variety of different sources generated over a range of conditions and temperatures. The geological and geochemical history of a conventional reservoir may have no direct relationship to the formational conditions of the trapped hydrocarbons. In contrast, gases in an unconventional reservoir are retained in the source and so experience the same thermal and burial history as the source rock after gas formation.

In both conventional and unconventional reservoirs, not all generated and/or trapped hydrocarbons are retained. For example, in thermally mature unconventional systems, the majority of generated hydrocarbons (including both oils and gases) are thought to be expelled over the course of oil and gas generation (e.g. Jarvie *et al.* 2007; Xia 2014). Similarly, in conventional systems if there is not a sufficient sealing lithology and trapping geometry then hydrocarbons will not be trapped. Thus, the gases trapped in both unconventional and conventional reservoirs may only represent a snapshot of the system's gas generation and accumulation history.

The second criterion we use to distinguish between various types of natural gas deposits is whether the gas was 'associated' (i.e. found) with or without liquid hydrocarbons in the reservoir. Associated or 'oil-associated' gases are either dissolved in oil ('solution gas') or present as a gaseous phase overlying a liquid phase in the reservoir (a 'gas cap'). 'Non-associated' gases are present in the gaseous phase in the reservoir and are not in contact with any liquid hydrocarbons in the subsurface. We apply a single-phase gas/oil ratio (GOR) of 6000 standard cubic feet/stock tank barrel (scf/stb) to differentiate non-associated gases in a subsurface accumulation from oil-associated gases. If there are two phases present in the subsurface (e.g. an oil leg with a gas cap), a 6000 scf/stb gas could be associated. While we recognize this here, we do not consider it further in this review.

There are additional classification schemes that use similar terms (oil-associated and non-associated) to indicate whether the gas was originally generated with oil or not (e.g. Schoell 1983). Other terms used to categorize and describe natural gas reservoirs include 'primary' gases that form directly from the breakdown of kerogen and 'secondary' gases that form via the breakdown of oil and hydrocarbon gases. These frameworks require *a priori* knowledge of the processes by and conditions under which a gas formed. Problematically, such information is generally not available and cannot always be inferred. Our usage of the terms conventional v. unconventional and associated v. non-associated are based solely on known conditions in

the reservoir at the time of drilling and hydrocarbon extraction. We note that in some cases a gas has been examined that is known to be thermogenic, but is not currently in a reservoir (e.g. a gas seep). Such gases are included in the larger comparison of thermogenic and biogenic gases, but not in the more specific comparisons of different types of thermogenic gases. The locations of the various accumulations are given in Figure 3.

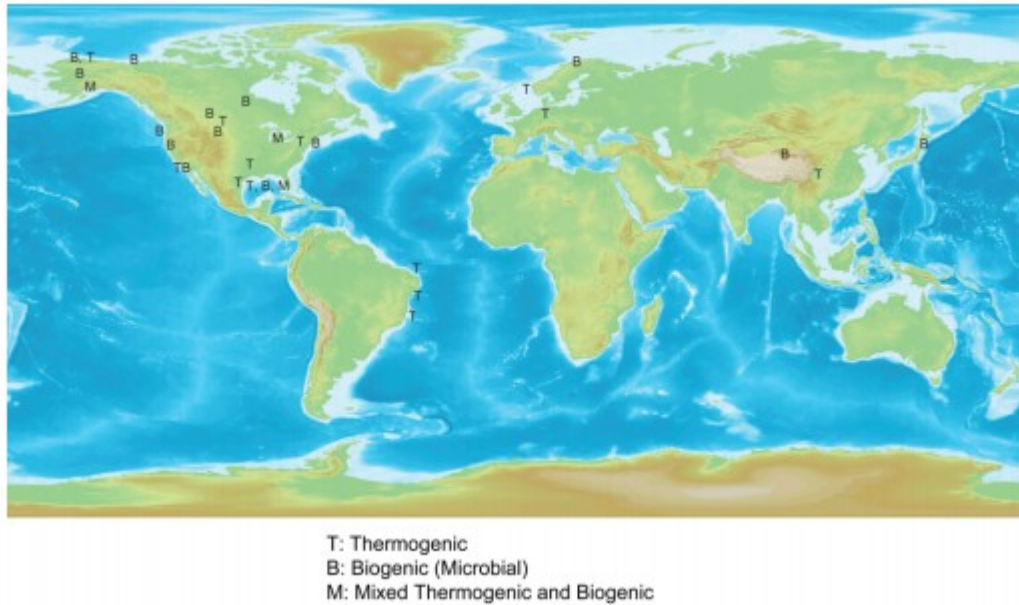


Fig. 3.

Locations of sampled gases discussed here. Data derived from Stolper *et al.* (2014a, 2015), Wang *et al.* (2015), Inagaki *et al.* (2015), Douglas *et al.* (2016, 2017) and Young *et al.* (2017). Specific accumulations and locations are discussed in these references.

### The first thermogenic methane clumped-isotope results

The first evidence that methane clumped-isotope measurements may yield meaningful gas-formation temperatures came from Stolper *et al.* (2014b). Specifically, isotopic (including clumped-isotope) measurements were made on methane sampled from a commercial high-purity gas cylinder. Based on its bulk isotopic composition ( $\delta D = -175.5\text{‰}$  and  $\delta^{13}C = -42.9\text{‰}$ ), the sample was assumed to be thermogenic in origin (Fig. 1a). Methane from the cylinder yielded a clumped-isotope temperature of  $170^{\circ}C$ . This temperature is within the range expected for thermogenic gas-formation temperatures (c.  $60\text{--}300^{\circ}C$ ; e.g. Behar *et al.* 1992; Hunt 1996; Tsuzuki *et al.* 1999; Vandenbroucke *et al.* 1999; Tang *et al.* 2000; Dominé *et al.* 2002; Burruss & Laughrey 2010) and is thus a geologically reasonable gas-formation temperature. Following this, additional measurements of gases from cylinders or laboratory gas lines with assumed thermogenic origins (again based on bulk isotopic compositions) using the spectroscopic technique yielded clumped-isotope-based temperatures from  $151$  to  $212^{\circ}C$  (Ono *et al.* 2014). These results are consistent with methane clumped-isotope temperatures reflecting thermogenic gas-formation temperatures, but, due

to lack of knowledge of the samples' origins, they could not be evaluated further.

Stolper *et al.* (2014a) presented the first methane clumped-isotope measurements of thermogenic gases from experimental simulations of thermogenic gas generation and from samples taken from unconventional non-associated and conventional oil-associated gas deposits. For reasons discussed above, unconventional deposits were targeted because the thermal history of the gas (once formed) and the source/reservoir are identical.

Non-associated gases extracted from unconventional deposits hosted in the Haynesville Shale (Texas; Hammes *et al.* 2011) and Marcellus Shale (Pennsylvania; Lash & Engelder 2011) were studied. The Haynesville Shale deposits currently remain near their maximum burial depths and temperatures (Stolper *et al.* 2014a). The measured clumped-isotope temperatures ranged from 169 to 207°C and are within  $2\sigma$  of the measurement precision of current reservoir temperatures (163–190°C), modelled maximum burial temperatures (175–207°C), and independently modelled gas-formation temperatures (168–173°C; Fig. 4; Stolper *et al.* 2014a). It is important to note here that the methane clumped-isotope temperatures of gases sampled from a subsurface hydrocarbon accumulation reflect the bulk weighted average temperature of all methane that was generated and stored (i.e. it is a cumulative measure).

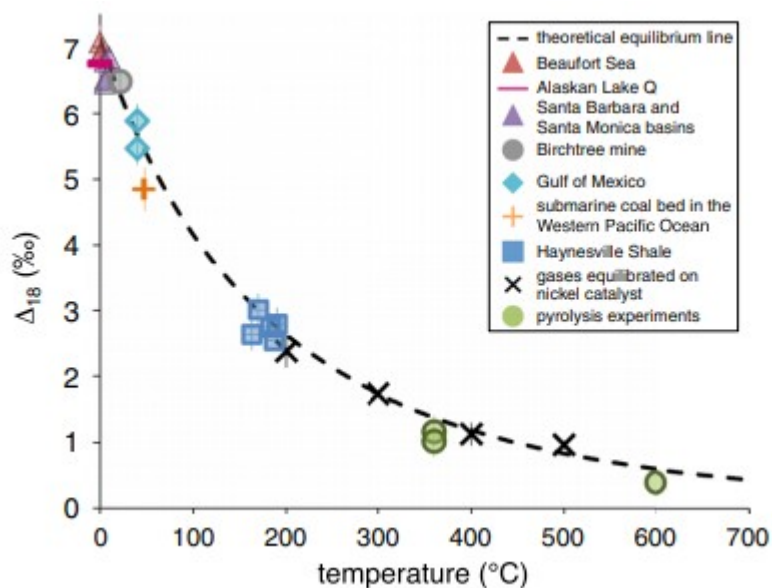


Fig. 4.

Samples of biogenic and thermogenic gases from environmental systems or experimental products with independently constrained formation temperatures (given by the x-axis) compared to measured  $\Delta_{18}$  values. Data from Stolper *et al.* (2014a, b, 2015), Inagaki *et al.* (2015), Douglas *et al.* (2016) and Young *et al.* (2017). Data from Inagaki *et al.* (2015) and Young *et al.* (2017) were converted to the  $\Delta_{18}$  reference frame based on  $\Delta^{13}\text{CH}_3\text{D}$  temperatures. Error bars are  $1\sigma$ .

In contrast to the Haynesville Shale, the section of the studied Marcellus Shale reached maximum burial temperatures, which are modelled to have been between 183 and 219°C, and then was uplifted and cooled to current temperatures between 60 and 70°C (Stolper *et al.* 2014a). The clumped-isotope temperatures for these Marcellus Shale samples were found to range from 179 to 207°C (Stolper *et al.* 2014a). This range overlaps the Haynesville Shale clumped-isotope temperature range and all measured temperatures are within 2 $\sigma$  of model-based average gas-formation temperatures (171–173°C).

Although these clumped-isotope temperatures are consistent with expected gas-formation temperatures in the studied Haynesville and Marcellus Shale samples, an alternative interpretation is that the temperatures reflect partially or completely the effects of isotope-exchange reactions that occurred after gas formation. In other words, if methane, after formation, continued to isotopically re-equilibrate, the clumped-isotopic composition would reflect the gas's thermal history post formation. Re-equilibration would require methane to exchange hydrogen isotopes with methane molecules or other compounds including, for example, H<sub>2</sub>O, H<sub>2</sub> or other hydrogen-bearing compounds. The rate of this exchange will scale with temperature, with faster rates at higher temperatures. The temperature below which such reactions cease to occur at a significant rate is termed an isotopic 'blocking temperature.' Such blocking temperatures have been studied previously for carbonate clumped isotopes (e.g. Ghosh *et al.* 2006; Dennis & Schrag 2010; Passey & Henkes 2012; Stolper & Eiler 2015). The clumped-isotope results from the Marcellus and Haynesville Shale samples indicate that the methane clumped-isotope blocking temperature in these unconventional deposits is above the shales' maximum burial temperatures (>200°C). Specifically, if the methane clumped-isotope blocking temperature was less than 200°C for geologically relevant timescales, the Marcellus Shale samples would presumably have yielded clumped-isotope-based temperatures consistently lower than the Haynesville Shale samples due to uplift and cooling of the examined Marcellus Shale gases after gas generation. This was not observed. We note though, that the blocking temperatures for methane, whatever they are, may and likely will vary based on the mineralogy of the reservoir rock (e.g. presence of transition metals like nickel) and chemical conditions (e.g. presence or absence of H<sub>2</sub>O or oil) in the reservoir (Seewald 2003). Such different conditions will affect the reaction pathways available to promote C–H exchange.

Taken together, the clumped-isotope temperatures from the Haynesville and Marcellus Shale samples reported by Stolper *et al.* (2014a) represent geologically reasonable temperatures for thermogenic gas formation. They appear unaffected by subsequent cooling of the systems and agree with independent metrics and models for thermogenic gas-formation temperatures (e.g. Tissot & Welte 1978; Quigley & Mackenzie 1988; Hunt 1996; Seewald *et al.* 1998; Seewald 2003). Thus, the measured clumped-

isotope temperatures are, to first order, conceivable average gas-formation temperatures. This was explored further in Stolper *et al.* (2014a) with measurements of oil-associated thermogenic gases from a conventional reservoir in the Potiguar Basin, Brazil. Methane from Potiguar Basin samples yielded clumped-isotope temperatures from 157 to 221°C. These temperatures are also in the expected range of thermogenic gas-formation temperatures. Additionally, the clumped-isotope temperatures correlated positively with the  $\delta^{13}\text{C}$  values of methane – such a correlation was expected based on conventional interpretations of  $\delta^{13}\text{C}$  as a maturity indicator (discussed in the sections entitled ‘Conventional molecular and isotopic techniques used to study the origins of hydrocarbon gases’ briefly above and ‘Values of  $\delta^{13}\text{C}$  and clumped-isotope temperatures of thermogenic gases’ more extensively below).

It is noteworthy that some methane clumped-isotope temperatures from the Potiguar Basin samples, all of which are oil-associated, fall outside of the commonly assumed temperature range for oil generation (the oil window) of c. 60 to 160°C (Hunt 1996) and even more recent maximum estimates of c. 200°C; (e.g. Vandembroucke *et al.* 1999; Lewan & Ruble 2002). Stolper *et al.* (2014a) proposed that the ‘hot’ methane did not form with oil but instead, during migration, ended up in the same reservoir as the oil. Indeed, source rocks of high maturity (past oil-window maturity) are found in the Potiguar Basin, making such an idea plausible (Stolper *et al.* 2014a). As will be discussed in the next section, thermogenic gases from different hydrocarbon systems frequently yield methane clumped-isotope temperatures from 60 to 160°C indicating methane clumped-isotope temperatures consistent with co-formation of gas and oil are common.

Finally, clumped isotopes were measured on methane generated experimentally by closed-system hydrous pyrolysis of organic-rich shale at 360°C or closed-system anhydrous pyrolysis of pure propane at 600°C. The temperatures were found to be within  $2\sigma$  measurement precisions of the known formation temperatures. Additionally, these temperatures were  $5\sigma$  away from measured clumped-isotope temperatures from environmental thermogenic methane samples (Fig. 4). These experiments thus independently support the hypothesis that methane clumped-isotope temperatures can reflect formation temperatures. In all, these results led Stolper *et al.* (2014a) to hypothesize that clumped-isotope-based temperatures of thermogenic gases could be used to infer, at least for the systems examined, average gas-formation temperatures.

Further studies of thermogenic gases

Additional clumped-isotope studies of thermogenic gases from a variety of different hydrocarbon systems have now been made (e.g. Stolper *et al.* 2015; Wang *et al.* 2015; Douglas *et al.* 2016, 2017; Young *et al.* 2017). In this section we review the overall distribution of clumped-isotope-based temperatures derived from thermogenic gases (study locations given in Fig.

3). All measured thermogenic conventional oil-associated and non-associated gases and unconventional non-associated gases are included. Unconventional oil-associated gases appear to yield non-equilibrium clumped-isotope distributions and are not included in the present discussion. They are treated separately below. The geological and production histories can be found in the original studies from which the measurements are taken (see Douglas *et al.* 2017).

The observed range of clumped-isotope temperatures for thermogenic methane is from 72 to 298°C (Fig. 5c). The temperatures are normally distributed with a peak value of 175°C ± 47°C (1σ; Fig. 5c). This distribution can be compared to model-based expectations for both the expected range of methane formation temperatures and the amount of methane produced as a function of temperature. In models of methane generation, the amount of methane produced at different temperatures varies because it is assumed that rates of methane generation increase with increasing temperature but decrease as methane precursors are converted to either methane or oxidized forms of carbon such as graphite (Seewald 2003).

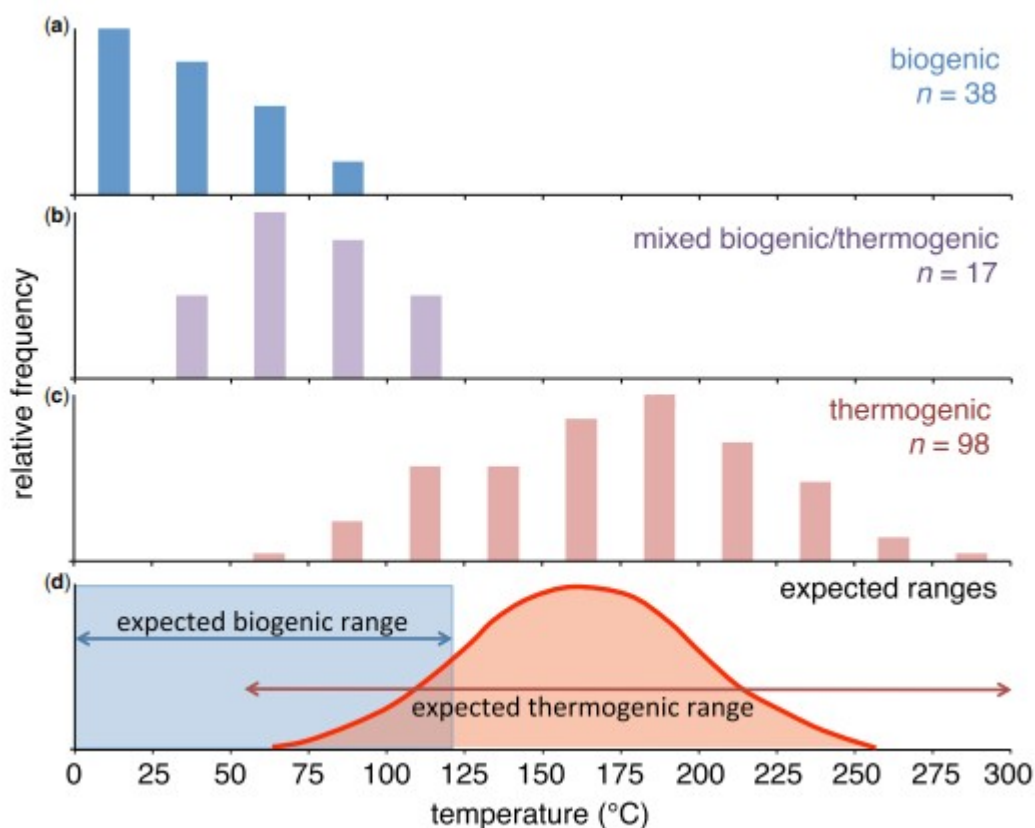


Fig. 5.

Distribution of measured clumped-isotope-based temperatures from biogenic (a), mixed thermogenic and biogenic (b) and thermogenic (c) gases compared to expected formation ranges of biogenic and thermogenic gases (d); the thermogenic distribution is derived from Hunt (1996). Data from Stolper *et al.* (2014a, 2015), Wang *et al.* (2015), Inagaki *et al.* (2015), Douglas *et al.* (2016, 2017) and Young *et al.*

(2017). Number of samples measured is given by  $n$ . All histograms are normalized such that the maximum box has a height of 1.

We use the model of Hunt (1996), which is reproduced in Figure 5d, to make the comparison between measured v. expected gas-formation temperatures and the expected distribution of those temperatures. The model of Hunt (1996) is a general model of methane generation kinetics. We note, though, that there are other models of gas generation distributions as a function of temperature and they do not always agree (e.g. Seewald 2003). Regardless, the overall range and distribution of measured v. modelled temperatures are similar indicating that the two are in general agreement. We note that direct comparisons of all measured thermogenic gas clumped-isotope-based temperatures with modelled formation temperatures and thermal burial histories of the source rocks, as was done for unconventional unassociated gases in Stolper *et al.* (2014a), is not generally possible. This is because most examined samples do not have independently constrained thermal and generation histories (e.g. because they have migrated from their source rock to the reservoir rock and/or lack independent constraints to calibrate a model of their thermal histories), thus preventing such a comparison.

The measured clumped-isotope temperatures extend to higher temperatures (c. 300°C) than the c. 250°C cut-off indicated by the model of Hunt (1996). However, recent models, the discovery of high-temperature oil reservoirs, and experiments all indicate that oils can be stable up to c. 200°C (e.g. Tsuzuki *et al.* 1999; Vandenbroucke *et al.* 1999; Lewan & Ruble 2002) and that methane generation occurs at temperatures above 250°C in nature (e.g. Behar *et al.* 1992; Tsuzuki *et al.* 1999; Vandenbroucke *et al.* 1999; Tang *et al.* 2000; Dominé *et al.* 2002; Burruss & Laughrey 2010). Although the maximum temperature of thermogenic methane generation remains an open question, the clumped-isotope temperatures are in line with these recent indications that it may extend up to at least c.300°C. Alternatively, these higher temperatures could result from subtle kinetic isotope effects expressed during gas generation or migration.

Specifically, recent pyrolysis experiments on coal (Shuai *et al.* in press) indicate that disequilibrium effects can be expressed during methane generation. In these experiments coal was heated in sealed gold tubes at different rates (i.e. increase in temperature per unit time) to a final temperature between 400 and 620°C. Samples quenched between 400 and 520°C yield  $\Delta_{18}$  values consistent with the generation of methane at equilibrium. Above 520°C,  $\delta D$  values increase rapidly and  $\Delta_{18}$  values first decrease (becoming negative) and then increase at 600°C to  $\Delta_{18}$  values similar to those expected for clumped-isotope equilibrium for the final experimental temperature. These  $\Delta_{18}$  values indicate that non-equilibrium processes during methane generation can occur at elevated temperatures in experimental samples. Interestingly, the transition to non-equilibrium  $\Delta_{18}$  values coincides with the onset of ethane cracking. The precise mechanisms controlling the non-equilibrium  $\Delta_{18}$  values of the evolved methane are

currently unknown, nor is it clear whether they are relevant to natural systems. However, they show that laboratory pyrolysis experiments can create both equilibrium and non-equilibrium methane clumped-isotope compositions depending on the details of the experiment.

The following sections focus on how the clumped-isotope temperatures reflect both the formational conditions and trapping histories of oil-associated and non-associated gases in conventional and unconventional reservoirs. We do not discuss cases where the origin of the thermogenic gases is not well constrained (e.g. thermogenic gas seeps).

### Conventional oil-associated gases

Oil-associated methane trapped in conventional reservoirs (from six distinct hydrocarbon systems) yield clumped-isotope temperatures that range from 103 to 266°C, with an average value of 167°C ( $\pm 40^\circ\text{C}$ ,  $1\sigma$ ; Fig. 6a). This range spans nearly the entire expected range of thermogenic gas generation temperatures (Fig. 6a v. Fig. 6e). Clumped-isotope temperatures of oil-associated gases from conventional reservoirs are equally common from 100 to 150°C as 150 to 225°C, with a sharp drop-off in frequency for temperatures above 225°C (Fig. 6a). Thus, the examined oil-associated gases, to first order, yield temperatures consistent with generation in the oil window ( $< c. 160^\circ\text{C}$ ) and at temperatures above oil stability. The overall range of clumped-isotope temperatures is probably the result of the capacity for conventional reservoirs to trap hydrocarbons generated over the full spectrum of potential gas generation temperatures. For example, if the gases in the reservoir were co-generated with the oils and remained associated during migration, the methane clumped-isotope temperatures might be expected to range from about 60 to 160°C. However, if the reservoirs also capture gases generated at higher temperatures (e.g. from the breakdown of oil and gas or kerogen above the oil window), then the measured methane clumped-isotope temperatures could be higher. Indeed, as some models predict that most natural gas forms above oil generation temperatures ( $>150^\circ\text{C}$ ; Quigley & Mackenzie 1988), it may not be surprising that conventional reservoirs often contain methane with clumped-isotope temperatures above 150°C.



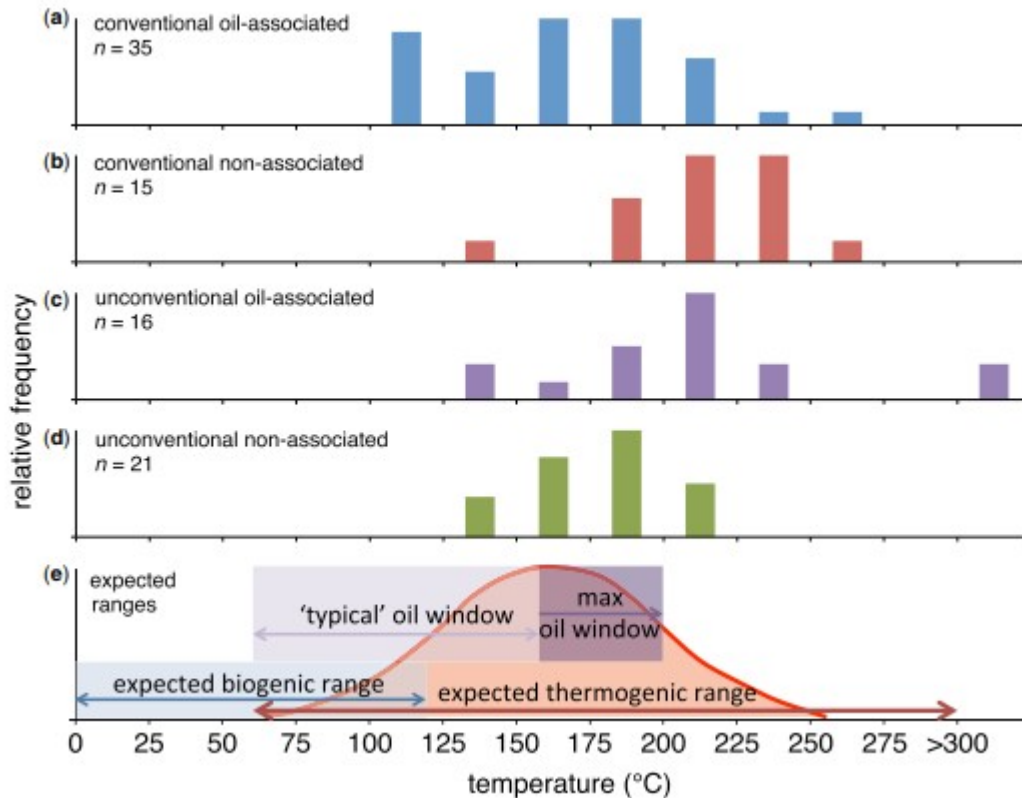


Fig. 6.

Distribution of measured clumped-isotope-based temperature from thermogenic deposits including: (a) conventional oil-associated deposits; (b) conventional non-associated deposits; (c) unconventional oil-associated deposits; and (d) unconventional non-associated deposits. These are compared to expected formation ranges of biogenic and thermogenic gases in (e). Data from Stolper *et al.* (2014a, 2015), Wang *et al.* (2015), Young *et al.* 2017 and Douglas *et al.* (2017). Number of samples measured is given by  $n$ . All histograms are normalized such that the maximum box has a height of 1. The typical range of oil generation is often given from c. 60 to 160°C (Hunt 1996), but some models indicate that oils can be generated and are stable up to c. 200°C (Tsuzuki *et al.* 1999; Lewan & Ruble 2002). Other ranges are described in Figure 5.

An alternative interpretation for the observed temperature ranges measured in conventional oil-associated gases is that they contain a component of methane formed in equilibrium and a component formed with  $\Delta_{18}$  values lower than expected for isotopic equilibrium, as occurs in some coal-pyrolysis experiments (Shuai *et al.* in press). We do not favour this interpretation for the data summarized in Figure 6a for two reasons: (1) methane in conventional oil-associated deposits has not yielded clumped-isotope temperatures that exceed plausible gas generation temperatures (unlike the non-equilibrium temperature intervals of the pyrolysis experiments discussed above or some of the more extreme findings for unconventional oil-associated gases described below); and (2) correlations between  $\delta^{13}\text{C}$  and methane temperature in the conventional oil-associated gases (presented below) generally resemble those expected for models of isotopic evolution during petroleum generation.

The observed range in clumped-isotope temperatures in conventional oil-associated deposits suggests one use of clumped-isotope measurements of methane is to establish whether the gases present in the deposit were co-generated with the oil or formed later (e.g. from the cracking of residual oil in the source rock, from oil in deeper reservoir intervals, or from a different source interval entirely) and mixed into the oils during migration. As will be discussed below (section entitled 'A synthesis of clumped-isotope studies and their utility in the study of economic accumulations of hydrocarbons'), this information can be used in an exploratory framework to detect the generation of hydrocarbons at greater depths and higher temperatures than oil generation, even in systems where the deeper-formed gas has dissolved into oils at shallower depths. Such information could indicate the potential for gas reservoirs at greater depths.

#### Conventional non-associated gases

Methane clumped-isotope measurements have been made on conventional non-associated gases from two systems. The first is the Rotliegend system in Germany (McCann 1998), where gases are coal-derived (a 'type III' kerogen source): see, for example, Killips & Killips (2013) or Peters *et al.* (2005) for further explanation on kerogen types. The second is from the North Sea (Sleipner Vest; mixture of algal [type II] and coal [type III] sources; Ranaweera 1990). Together, these systems yield an average clumped-isotope temperature of 213°C ( $\pm 30$ ,  $1\sigma$ ; Fig. 6b) with a range from 144 to 267°C. More specifically, the Rotliegend samples have an average temperature of 217°C ( $\pm 34$ ,  $1\sigma$ ) and the North Sea samples have an average temperature of 205°C ( $\pm 21$ ,  $1\sigma$ ).

These average clumped-isotope temperatures are higher than the average for conventional oil-associated gases (167°C). Indeed, only one sample (from Rotliegend) yields a temperature (144°C) consistent with generation below the oil window (<160°C). A simple interpretation of this result is that these hydrocarbon reservoirs captured gases dominantly generated at temperatures above oil generation. If broadly applicable, this would indicate that the majority of non-associated gases form at temperatures above oil generation. This hypothesis will require the examination of a wider range of conventional non-associated gases.

Alternatively, the difference between the clumped-isotope temperatures of conventional oil-associated v. non-associated gases may be due to different source organic types. The oil-associated gases were sourced dominantly from lacustrine and marine, organic carbon (type I and II kerogens). In contrast, the non-associated gases are sourced in part from dominantly gas-prone coals (type III kerogens). Some experiments indicate that gas generation kinetics for coals v. marine and lacustrine sources can differ (e.g. Burnham 1989; Pepper & Dodd 1995; Behar *et al.* 1997) and that coals yield methane at higher temperatures than other kerogen types (e.g. Pepper & Dodd 1995; Behar *et al.* 1997). Thus, the higher average temperatures in the

studied non-associated conventional gases relative to associated gases may result from different kerogen sources.

#### Unconventional non-associated gases

Methane clumped-isotope temperatures from unconventional non-associated gases (sampled from five different basins) have an average value of 179°C ( $\pm 23^\circ\text{C}$ ,  $1\sigma$ ; Fig. 5d) and range from 144°C to 207°C. All temperatures are at the top or above the nominal oil window (c. 160°C). Because gases in unconventional systems are thought to have formed *in situ* (Curtis 2002), the clumped-isotope temperatures, if interpreted as average gas-formation temperatures, indicate that these systems retain gases dominantly formed after oil generation either from oil, gas, or residual kerogen cracking.

The higher average temperature and tighter distribution (smaller standard deviation) of unconventional non-associated gases compared to oil-associated gases are consistent with the trapping histories of these different reservoir types. Specifically, unconventional systems retain the gases formed within the reservoir. Additionally, these systems are thought, in many cases, to expel oil and gas formed during oil generation at lower temperatures (e.g. Jarvie *et al.* 2007; Xia 2014), which would release methane formed at lower temperatures during oil generation ( $<160^\circ\text{C}$ ). After any such expulsion event(s), the system would then preferentially retain gases formed either from oil and gas cracking or the breakdown of residual kerogen at temperatures above 160°C. This does not indicate that all non-associated unconventional systems only retain higher-maturity gases, but that those that have been examined, which are economically productive, appear to preferentially sample gases with higher ( $>150^\circ\text{C}$ ) clumped-isotope temperatures. The clumped-isotope temperatures of non-associated gases from unconventional reservoirs could be used to place quantitative constraints on the timing and mass of oil and gas expelled from the unconventional reservoir. This requires incorporating methane clumped-isotope temperatures into current quantitative models of oil and gas generation.

We note that clumped-isotope temperatures of methane from non-associated unconventional reservoirs do not yield the elevated temperatures ( $>220^\circ\text{C}$ ) we observe in some conventional accumulations. It is possible that this is simply the result of the specific unconventional systems that have been studied to date, which, where known, do not exceed modelled maximum burial temperatures greater than 220°C (Stolper *et al.* 2014a). Future studies could focus on comparing conventional gas accumulations sourced from shales that are currently unconventional to the gases still retained in the shale.

An observation that we discuss below is that the samples with the most enriched  $\delta^{13}\text{C}$  values for methane (i.e. greater than  $-32\text{‰}$ ), which are generally taken to indicate generation at elevated maturities and thus higher temperatures, do not have the highest clumped-isotope-based temperatures.

Instead, these samples yield clumped-isotope temperatures that are commonly c. 150°C. This is unexpected if clumped-isotope-based temperatures are interpreted as average formation temperatures. We return to this intriguing discrepancy below (section entitled 'Values of  $\delta^{13}\text{C}$  and clumped-isotope temperatures of thermogenic gases') when plots of  $\delta^{13}\text{C}$  v. clumped-isotope temperatures are discussed in detail.

#### Unconventional associated gases

Two unconventional reservoirs with oil-associated gases have been studied: the Eagle Ford Shale (Texas; Mullen 2010), and the Bakken Shale (North Dakota; Meissner 1978). The presence of oil in these systems constrains the maximum formation temperatures of the methane to temperatures below those at which oil is stable on geological timescales. Although this temperature is not agreed upon, it is probably no higher than c. 200°C under geological conditions (Quigley & Mackenzie 1988; Hunt 1996; Vandenbroucke *et al.* 1999; Lewan & Ruble 2002). In contrast, the clumped-isotope temperatures of gases from these reservoirs range from 140 to 380°C, with an average value of 215°C ( $\pm 59$ ,  $1\sigma$ ). Thus, many of the measured temperatures exceed what would be expected for oil stability. Furthermore, the temperatures are higher, on average, than unconventional non-associated gases, which are derived from systems modelled in many cases to have reached burial temperatures above 200°C. This strongly indicates that the clumped-isotope compositions of the unconventional oil-associated deposits studied do not reflect equilibrium conditions during gas generation. Instead they probably reflect kinetic isotope effects expressed during methane generation, storage in the reservoir (including leakage or phase changes), or extraction of hydrocarbons.

Kinetic isotope effects expressed during gas generation could have created the observed non-equilibrium clumped-isotope compositions. Evidence in favour of this possibility comes from pyrolysis experiments on coal discussed above which result in lower  $\Delta_{18}$  values (and thus hotter apparent temperatures) during some experimental conditions. If this process occurs in natural environments it could explain the high apparent methane clumped-isotope temperatures from the Eagle Ford and Bakken formations. This scenario requires that the kinetics and reaction mechanisms for gas generation in these unconventional systems differ from other systems which do not yield such high apparent clumped-isotope temperatures, but instead temperatures generally consistent with generation in the oil window. This is because a significant proportion (35%) of all thermogenic gases yield clumped-isotope temperatures less than 160°C, i.e. below the typically assumed maximum range for the oil window (Fig. 6a).

Finally, we note that although the coal-pyrolysis experiments only yield non-equilibrium  $\Delta_{18}$  values at the onset of ethane cracking, ethane is considered the second most stable alkane (with methane the most stable) with respect to thermally activated breakdown reactions (Behar *et al.* 1992). For

geologically relevant thermal histories, ethane breaks down only after oil has cracked to hydrocarbon smaller gases (Behar *et al.* 1992). Thus, the relevance of the experiments to oil-associated, unconventional gases is not clear.

Alternatively, the non-equilibrium clumped-isotope compositions could result from kinetic isotope effects expressed during gas extraction. The extraction of gas and oil from conventional systems v. unconventional systems can differ. Specifically, unconventional systems are usually hydraulically fractured in order to release hydrocarbons whereas most conventional reservoirs are not. During oil and gas recovery from unconventional reservoirs, the pressure in the reservoir declines rapidly over the first year, lowering the total yield of oil and gas that can be extracted over time (e.g. Lee *et al.* 2011). Larger molecules such as liquid hydrocarbons require larger pressure gradients for recovery compared to gases. Thus, it is possible that oils that contain some dissolved methane are left behind in the reservoir during production of hydrocarbons or that a two-phase hydrocarbon system develops within the subsurface if the pressure in the reservoir drops below the bubble point. Nonetheless, kinetic isotope effects associated with the dissolution or degassing of methane into or out of this oil could result in the observed non-equilibrium clumped-isotopic compositions of the methane. The apparently meaningful gas-formation temperatures from unconventional non-associated systems in which methane is the dominant constituent and no oil is presented supports this idea. This hypothesis could be tested by taking samples from a well at different times in its production history as the pressure in the unconventional reservoir declines.

Additionally, kinetic isotope effects may be expressed during the migration of gases from the shale into the fractures created during hydraulic fracturing of the shales. For example both diffusion and adsorption/desorption of hydrocarbons are thought to occur during migration in shales and could result in the expression of kinetic isotope effects (Xia & Tang 2012). If such kinetic isotope effects are preferentially expressed when oil is present in a system (e.g. because a liquid hydrocarbon phase changes the isotope effects associated with methane's diffusivity or sorption behavior), they could influence the methane clumped-isotope compositions. Regardless of this, future work on oil-associated unconventional deposits should focus on understanding why these gases show different clumped-isotope systematics as compared to higher-maturity unconventional deposits and conventional reservoirs.

Thermogenic methane in clumped-isotopic equilibrium?

The bulk isotopic composition (i.e.  $\delta D$  and  $\delta^{13}C$ ) of thermogenic methane is generally considered to be set by kinetically controlled processes (Sackett 1978; Chung *et al.* 1988; Clayton 1991; Tang *et al.* 2000; Ni *et al.* 2011). Only at the highest gas maturities (temperatures  $>200^{\circ}C$ ) have equilibrium exchange processes between methane and water been suggested to

influence the  $\delta D$  values of thermogenic methane (Burruss & Laughrey 2010). However, year-long incubations of methane at 323°C in deuterium-labelled water do not result in the definitive occurrence of exchange of hydrogen isotopes between water and methane (Reeves *et al.* 2012). Nonetheless, it has generally been assumed that under most conditions, thermogenic methane's isotopic composition is controlled by kinetic isotope effects. Thus, the interpretation of some thermogenic methane clumped-isotope temperatures as gas-formation temperatures from 70 to 300°C requires the presence of unanticipated isotope-exchange processes during methane generation.

To explain this, we focus on mechanisms that could allow C-H bonds in methyl precursors to exchange hydrogen. It is important to note that achievement of C-H isotope equilibrium within methane or between methane and another phase does not require methane to be in carbon isotopic equilibrium with any other molecules during formation. It only requires reversible hydrogen isotope-exchange reactions to take place (perhaps only at a local molecular scale, such that evolved methane is still out of hydrogen isotope-exchange equilibrium with the bulk residue). Even so, it is possible for methane to be in internal isotopic equilibrium and still express kinetic carbon-isotope effects. We note that the framework of Helgeson *et al.* (2009), where hydrocarbons are hypothesized to be in metastable chemical equilibrium with each other and with CO<sub>2</sub>, may imply that carbon bonds could be breaking and forming between organic molecules. In such a case, the organic molecules could achieve carbon isotopic equilibrium both within and between organic species. Carbon-isotope equilibrium between different molecules in thermogenic deposits could be tested by comparing methane clumped-isotope temperatures to known carbon-isotope equilibrium compositions between methane and CO<sub>2</sub> or other hydrocarbons like ethane and propane (Singh & Wolfsberg 1975; Horita 2001). This has not been done but could serve as a test of the ideas of Helgeson *et al.* (2009).

One mechanism that could generate methane in internal isotopic equilibrium is via the isotopic pre-equilibration of methyl groups before methane generation via free radical migration in the backbone of the hydrocarbon precursors. As free radicals move from carbon atom to carbon atom, hydrogen atoms are added to and removed from the organic molecule. This process is how deuterium and hydrogen from water are thought to be incorporated into organic matter (Hoering 1984; Lewan 1997). If these hydrogen-exchange reactions proceed before C-C bond cleavage, the methyl groups could be in or near internal isotopic equilibrium before methane formation. Methyl groups and methane have been modelled to have similar clumped-isotopic compositions at internal isotopic equilibrium (Wang *et al.* 2015). Thus methane clumped-isotope compositions could partly reflect <sup>13</sup>C-D and D-D clumping in a methyl group precursor at the temperature of cleavage.

This hypothesis requires that hydrogen addition to a released methyl group allows this internal equilibrium to be maintained. Alternatively, hydrogen isotope-exchange reactions available to the methyl free radical could promote internal isotopic equilibrium. This could occur through catalytically induced exchange reactions of methane or methyl groups during formation on other phases including clays, organic surfaces or transition metals. For example, clays have been experimentally demonstrated to catalyse hydrogen exchange in larger organic molecules (Alexander *et al.* 1982, 1984) while transition metals (Mango *et al.* 1994; Mango & Hightower 1997) have been implicated in the catalysis of methane generation. In laboratory experiments, transition metals like nickel and platinum can equilibrate the hydrogen isotopes of methane and H<sub>2</sub> (Horibe & Craig 1995) and allow methane to achieve internal isotopic equilibrium at temperatures above 150°C (Ono *et al.* 2014; Stolper *et al.* 2014b).

Regardless of mechanism, in order for thermogenic methane clumped-isotope compositions to reflect gas-formation temperatures, methane must form in internal isotopic equilibrium and retain that signature after formation. Thus, the processes that allow methane to form in clumped-isotopic equilibrium cannot promote the continued isotopic equilibration after formation. If correct, this indicates that hydrogen-isotope exchange reactions for methyl precursors or during methane generation exist, but cease to be available to methane after it is formed.

## Biogenic gases

### Biogenic gases in clumped-isotopic equilibrium

Stolper *et al.* (2014a) presented the first methane clumped-isotope measurements from biogenic sources. Biogenic methane from kilometre-deep reservoirs in the Gulf of Mexico undergoing biodegradation and methane generation yielded methane clumped-isotope temperatures from 40 to 48°C, which are within 1 $\sigma$  measurement precision of the known reservoir temperatures of 42 to 48°C. Additionally, methane dominantly biogenic in origin (although with some contribution of thermogenic methane) from the Antrim Shale yielded a clumped-isotope temperature of 40°C. Based on these results (Fig. 4), Stolper *et al.* (2014a) hypothesized that clumped-isotope temperatures of biogenic methane can reflect gas-formation temperatures in some settings.

The correspondence between biogenic gas formation and clumped-isotope-based temperatures has been subsequently corroborated in other samples with independently known methane formation temperatures (Fig. 4). For example, measurements of biogenic methane seeps from the Santa Barbara and Santa Monica basins yield clumped-isotope temperatures between 6 and 16°C, within 2 $\sigma$  in all cases of the seep temperatures (5–9°C). Two measurements of biogenic methane from submarine coal beds yielded clumped-isotope temperatures of 70°C (with precisions of  $\pm 5$  and 12°C, 1 $\sigma$ ) in environments with temperatures from 45 to 50°C (Inagaki *et al.* 2015).

Samples emitted from underwater seeps on the Alaskan shelf in the Beaufort Sea have clumped-isotope temperatures from 0 to 5°C, all within 1σ error of local environmental temperatures (−1.5 to 0°C; Fig. 3; Douglas *et al.* 2016). Finally, a methane sample from the Birchtree nickel mine (Manitoba, Canada), which is thought to be biogenic in origin, yielded both - and -based temperatures of 16 ± 5 and 12 ± 2°C, similar to environmental temperatures of 20 to 23°C (Young *et al.* 2017).

Biogenic gases from systems without independently constrained gas-formation temperatures also yield clumped-isotope temperatures consistent with a biogenic origin. For example, biogenic methane from Northern Cascadia Margin methane clathrates yielded clumped-isotope-based temperatures between 12 and 42°C (Wang *et al.* 2015); coal-bed methane from the Powder River Basin has clumped-isotope temperatures from 35 to 52°C (Wang *et al.* 2015); and low, 9–30°C, clumped-isotope temperatures are observed in some gases collected from Alaskan lakes (Douglas *et al.* 2016).

Additional support for the hypothesis that biogenic gases can yield clumped-isotope temperatures that reflect generation temperatures comes from systems that are mixtures of biogenic and thermogenic gases or lack independent constraints on gas-formation temperatures. For example, in the Antrim Shale, gases are known to be a mixture of biogenic and thermogenic gases. In this system, gases independently interpreted to be dominantly biogenic (higher C<sub>1</sub>/C<sub>2-3</sub>) yielded lower clumped-isotope temperatures than gases enriched in ethane and propane (Fig. 7; Stolper *et al.* 2014a, 2015).

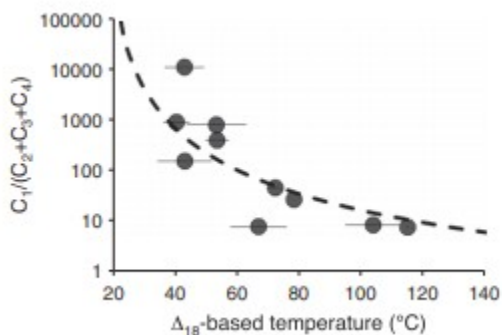


Fig. 7.

Clumped-isotope measurements from Antrim Shale deposits that contain a mixture of biogenic and thermogenic gases. As would be expected, samples with higher C<sub>1</sub>/(C<sub>2-4</sub>) ratios, which are more similar to the biogenic end member yield lower clumped-isotope-based temperatures and vice versa. Data are fitted to a model (dotted line) that includes mixing between a biogenic and thermogenic source with biological consumption of C<sub>2+</sub> alkanes. Data and the model are described fully in Stolper *et al.* (2015). Error bars are 1σ.

Taken together, along with measurements from other biogenic reservoirs (Douglas *et al.* 2016, 2017), some biogenic gases – specifically those that sample subsurface biogenic systems – show a range from −1 to 95°C (Fig. 5a). This range is within that generally expected for biogenic gases (<80°C;



Wilhelms *et al.* 2001; Valentine 2011) and well within maximum observed temperatures from laboratory pure cultures of up to 122°C (Fig. 5d; Takai *et al.* 2008). It further supports the hypothesis that biogenic methane can reflect gas-formation temperatures in many environmental settings.

### Biogenic gases out of isotopic equilibrium

Although some biogenic gases yield clumped-isotope-based temperatures consistent with their known formation temperatures, other samples both from the environment and from laboratory experiments do not. Specifically, methane generated by hydrogenotrophic methanogens in the laboratory (Stolper *et al.* 2014a, b; Wang *et al.* 2015; Young *et al.* 2017) and methylotrophic methanogens (Douglas *et al.* 2016; Young *et al.* 2017) universally yield non-equilibrium clumped-isotope-based temperatures. The calculated temperatures are either too hot compared to the laboratory growth temperatures or have negative  $\Delta_{18}$  or  $\Delta^{13}\text{CH}_3\text{D}$  values (Fig. 8). Negative  $\Delta_{18}$  or  $\Delta^{13}\text{CH}_3\text{D}$  values are impossible for a system in internal isotopic equilibrium. In environmental systems, biogenic methane from ponds (Stolper *et al.* 2015), mid-latitude lakes, cow rumens, ophiolites that generate sufficient  $\text{H}_2$  for methanogenesis to occur (Wang *et al.* 2015), Arctic lakes (Douglas *et al.* 2016) and various mines (Young *et al.* 2017) yield clumped-isotope temperatures that are unreasonably high or  $\Delta_{18}$  and  $\Delta^{13}\text{CH}_3\text{D}$  values that are negative.

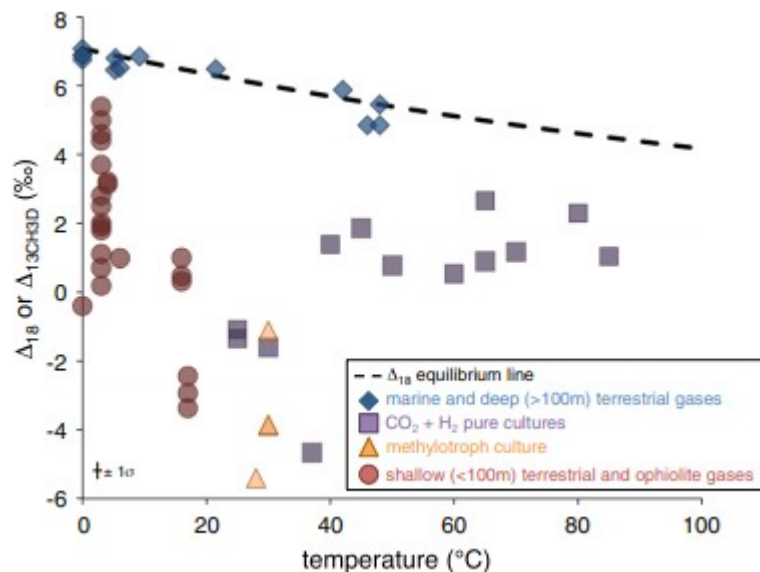


Fig. 8.

Comparison of measured  $\Delta_{18}$  or  $\Delta^{13}\text{CH}_3\text{D}$  values of biogenic gases to their known formational or environmental sampling temperatures. Marine and deep (>100 m) terrestrial gases yield  $\Delta_{18}$  values consistent with their formational temperatures. In contrast pure-culture hydrogenotrophic methanogens (that use  $\text{H}_2$  and  $\text{CO}_2$ ) and methylotrophic methanogens (that cleave methyl groups from larger organics), and biogenic methane from shallow terrestrial systems and ophiolites yield methane out of clumped-isotope equilibrium. Samples come from Stolper *et al.* (2014a, 2015), Wang *et al.* (2015), Inagaki *et al.* (2015), Douglas *et al.* (2016) and Young *et al.* 2017. Data from Inagaki *et al.*

(2015) and the Birchtree mine datum of Young *et al.* (2017) were converted to the  $\Delta_{18}$  reference frame using the  $\Delta^{13}\text{CH}_3\text{D}$ -based temperature to compare them to the equilibrium line (which is for  $\Delta_{18}$ ) as these samples were interpreted to have formed in clumped-isotope equilibrium. The typical  $1\sigma$  error bar for  $\Delta$  measurements is given in the figure.

What controls the clumped-isotopic compositions of biogenic methane?

Stolper *et al.* (2014a) proposed that the relative reversibility of the methanogenic enzymes (e.g. methyl co-enzyme M reductase) involved in biogenic methane generation could control the ultimate clumped-isotope composition of the gas. For example, high enzymatic reversibility would promote exchange of H and D in methane C-H bonds and allow biogenic methane to form in internal isotopic equilibrium. Stolper *et al.* (2015) and Wang *et al.* (2015) created quantitative models that could evaluate this hypothesis and found that the relative reversibility of enzymes could explain the biogenic clumped-isotope data. These models predict that non-equilibrium methane clumped-isotope values occur when enzymes are less reversible. The validity of these models is strengthened by their ability to relate differences in the hydrogen-isotopic composition of water and methane with the degree of disequilibrium for the clumped-isotope values.

The key insight provided by these models and environmental observations for the purposes of this review is that systems where growth rates are slow appear to show more reversibility in their enzymes (Valentine *et al.* 2004; Wing & Halevy 2014; Stolper *et al.* 2015; Wang *et al.* 2015) and thus create methane in clumped-isotopic equilibrium. Such systems (i.e. where growth rates are slow) would include marine sediments and deeply buried (e.g. >100 m deep) terrestrial systems – such systems tend to contain organic matter that is less reactive than organic matter found near the sediment-water interface. This less reactive organic carbon results in slower growth rates for the fermentative organisms that provide  $\text{H}_2$ , acetate and other methylated molecules to methanogens, lowering methanogen growth rates in the process. As many of these slow-growth systems occur at great depths (hundreds of metres to kilometres), where competent seals have the potential to develop, they could lead to the generation of biogenic gas accumulations in reservoir rocks above or within the locus of methanogenesis.

In contrast, systems in which methane generation rates (per cell) are high, show more irreversibility in their enzymes (Valentine *et al.* 2004; Wing & Halevy 2014; Stolper *et al.* 2015; Wang *et al.* 2015), and yield methane out of clumped-isotopic equilibrium. As discussed, this disequilibrium is manifested by lower  $\Delta_{18}$  values (i.e. higher clumped-isotope-based temperatures) than expected for isotopic equilibrium. Such systems tend to be found in shallow terrestrial settings, including lakes, wetlands, and ponds as well as in cow rumens, where large amounts of fresh, labile organic carbon are available for conversion by fermentative microorganisms to  $\text{H}_2$ , acetate and other methylated organic molecules used by methanogens (Stolper *et al.* 2015; Wang *et al.* 2015; Douglas *et al.* 2016). Such shallow systems are unlikely to

yield economic reservoirs of methane given the short transit distance to the atmosphere or sediment/water interface and the fact that sealing rocks are yet to develop the necessary competence to hold a significant column of free gas within a potential reservoir interval at such depths – this is discussed further below. Additionally, deeper terrestrial settings with large amounts of H<sub>2</sub> and CO<sub>2</sub> (or acetate), found for example in ophiolites, can also generate methane out of clumped-isotopic equilibrium (Wang *et al.* 2015).

#### Mixed biogenic and thermogenic deposits

Thermogenic gases generally yield clumped-isotope-based temperatures from 70 to 300°C. Biogenic gases from deeply buried marine or continental systems, on the other hand, yield clumped-isotope-based temperatures less than 100°C. Finally, shallowly sourced terrestrial systems yield variable temperatures, all of which are too hot for their given setting. Given these end-member compositions, a question is: can clumped-isotope-based temperatures be used to distinguish and quantify mixtures of biogenic gases and thermogenic gases?

Several economic hydrocarbon accumulations with contributions of both biogenic and thermogenic gases have been studied (Fig. 5b) and they yield temperatures that fall between the biogenic and thermogenic fields. Specifically, the clumped-isotope-based temperatures using data from economic deposits with mixtures of biogenic and thermogenic gases range from 40 to 118°C with an average of 73°C ( $\pm 25^\circ\text{C}$ ,  $1\sigma$ ). Importantly, in these examples, the biogenic gases appear to have formed at low metabolic rates such that the clumped-isotope-based temperatures and formation temperatures are similar for the biogenic end member. This probably indicates that in most economic hydrocarbon accumulations, the biogenic methane was formed close to isotopic equilibrium. For this comparison, we only included samples where the  $\delta\text{D}$  and  $\delta^{13}\text{C}$  values of the end members are sufficiently close such that mixing of gases results in a pseudo-linear dependence of clumped-isotope temperature on mixing ratio (Stolper *et al.* 2014a, b, 2015; Wang *et al.* 2015; Douglas *et al.* 2016). This generally requires that the end members do not differ by more than a few tens of per mille in their isotopic composition (although this generally has to be established on a case-by-case basis). Non-linear mixing of  $\Delta_{18}$  values occurs in the terrestrial Arctic as discussed below.

In these 'mixed' systems, clumped-isotope-based temperatures often correlate with other measured parameters that can differ between thermogenic and biogenic gases. For example, in the Antrim Shale, which contains mixtures of biogenic and thermogenic gases (Martini *et al.* 1996, 1998, 2003; Stolper *et al.* 2015), an inverse relationship between the clumped-isotope-based temperature and the C<sub>1</sub>/C<sub>2-3</sub> ratio is observed (Fig. 7). As discussed above, biogenic gases generally have higher C<sub>1</sub>/C<sub>2-3</sub> ratios than thermogenic gases. In the Antrim Shale, the clumped-isotope temperatures

were used to calculate the relative amounts of biogenic and thermogenic gases in samples taken from different wells (Stolper *et al.* 2015).

A distinctive scenario occurs when thermogenic and biogenic gases with significantly different  $\delta D$  and  $\delta^{13}C$  values mix. This scenario can occur in terrestrial settings in which both the  $\delta D$  and  $\delta^{13}C$  of the biogenic gases can be substantially lower (up to c. 200‰ for  $\delta D$  and c. 50‰ for  $\delta^{13}C$ ) compared to thermogenic gases (e.g. Whiticar *et al.* 1986). A mixture of two gases where one has significantly lower  $\delta D$  (hundreds of per mille) and  $\delta^{13}C$  (many tens of per mille) values than the other results in obvious non-linear mixing of  $\Delta_{18}$  values (Stolper *et al.* 2014a, b, 2015; Wang *et al.* 2015; Douglas *et al.* 2016). For such a mixture (i.e. where one end member has both lower  $\delta D$  and  $\delta^{13}C$  values than the other) the  $\Delta_{18}$  values of the mixture will be elevated (i.e. yield colder clumped-isotope temperatures) compared to a linear mixture of  $\Delta_{18}$  values. As a result, such mixtures can create non-physical, sub-freezing clumped-isotope-based temperatures. Examples of this sort of mixing scenario (including sub-freezing clumped-isotope temperatures) are given in Douglas *et al.* (2016) for terrestrial Alaskan samples. In the case of Douglas *et al.* (2016), these mixing relationships were corroborated using radiocarbon measurements where the thermogenic gases were radiocarbon-dead while the biogenic end member had measurable  $^{14}C$ . These sorts of mixing scenarios, especially when sub-freezing clumped-isotope-based temperatures are measured, identify the likely presence of thermogenic gases mixing into a shallow biogenic system.

Clumped-isotope temperatures in the context of Whiticar and Bernard plots

We now place samples with measured clumped-isotope compositions into the interpretive frameworks of the Whiticar and Bernard plots introduced earlier (Figs 9 & 10). To do this, we categorize samples as follows: biogenic gases are characterized as either 'non-equilibrium' or 'equilibrium' biogenic gases. 'Non-equilibrium' indicates that the clumped-isotope temperatures do not yield meaningful formation temperatures while 'equilibrium' indicates the clumped-isotope temperatures reflect meaningful formation temperatures. Thermogenic gases are separated as either conventional or unconventional and oil-associated or non-associated. Finally, we include gases that are a mixture of thermogenic and biogenic sources. Symbol fill colours represent the clumped-isotope based temperature. Blue colours indicate a lower clumped-isotope temperature while red colours indicate higher clumped-isotope temperatures. Gases with negative  $\Delta_{18}$  or  $\Delta^{13}CH_3D$  values or sub-freezing temperatures are coloured grey.

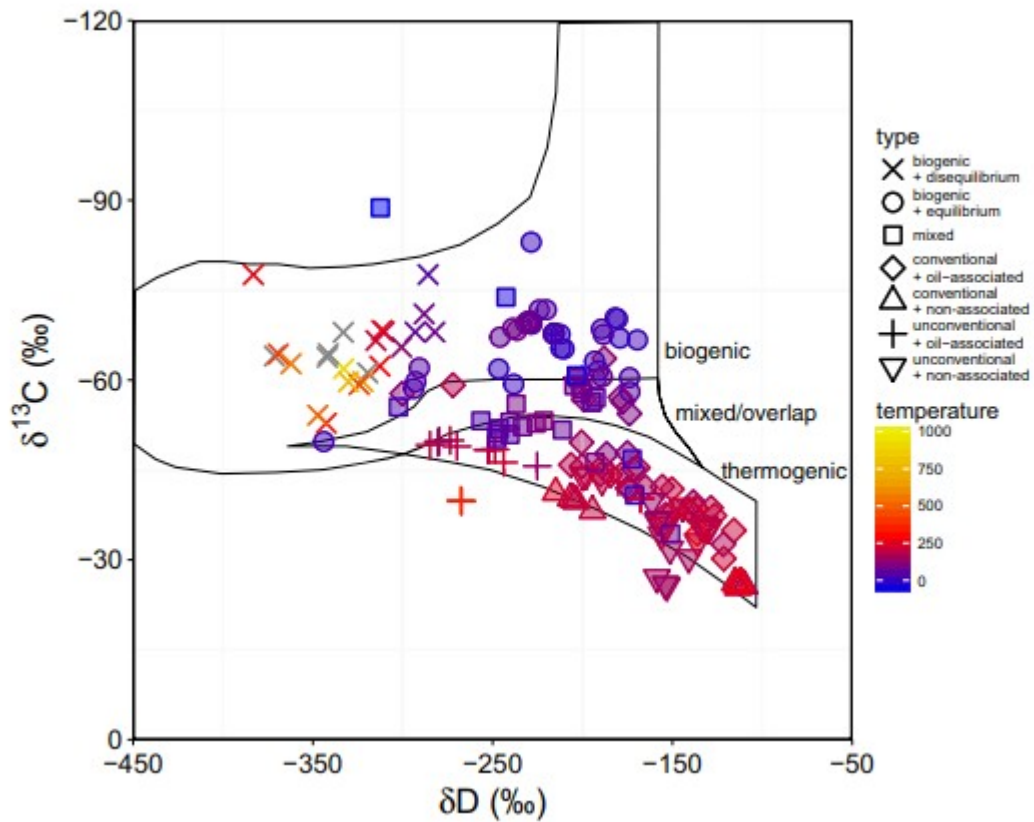


Fig. 9.

Comparison of measured clumped-isotope temperatures from samples of known origin to their position in the Whiticar plot (Whiticar *et al.* 1986; Whiticar 1999). Measured temperatures are indicated by the colour of the data point. Grey colours indicate either negative  $\Delta_{18}$  or  $\Delta^{13}\text{CH}_3\text{D}$  values or sub-freezing temperatures. Data from Stolper *et al.* (2014a, 2015), Wang *et al.* (2015), Inagaki *et al.* (2015), Douglas *et al.* (2016, 2017) and Young *et al.* (2017).

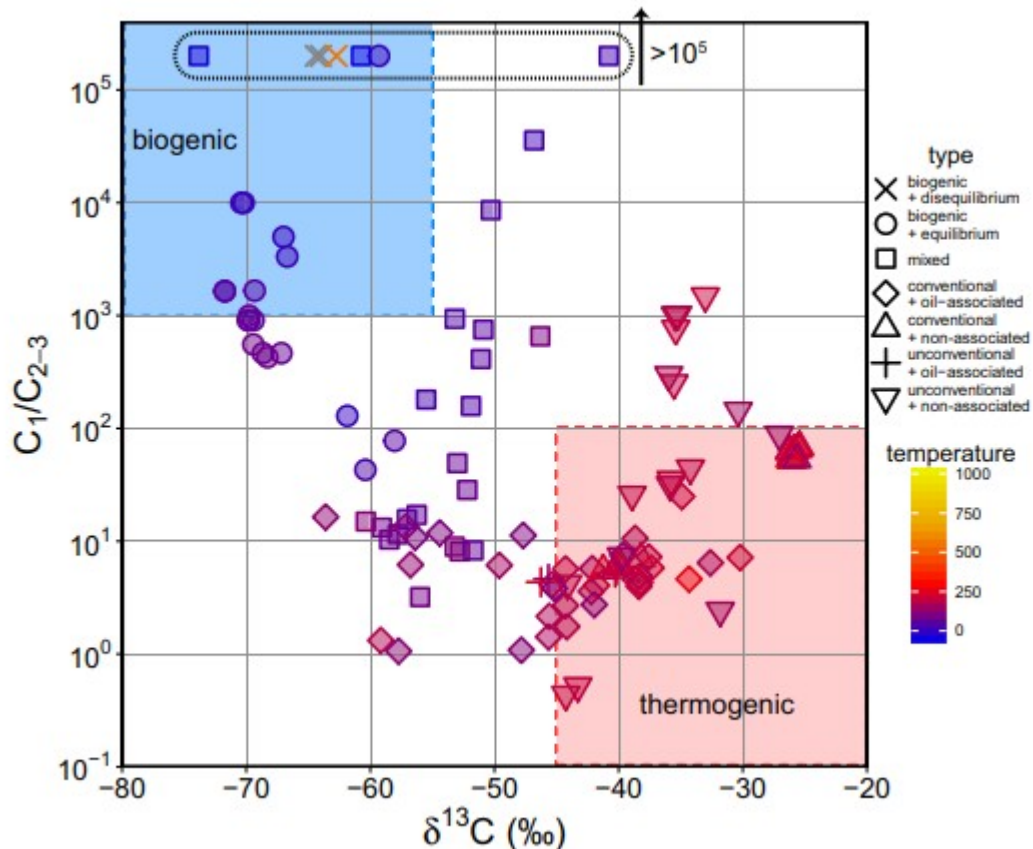


Fig. 10.

Comparison of measured clumped-isotope temperatures from samples of known origin to their position in the Bernard plot (Bernard *et al.* 1976). Measured temperatures are indicated by the colour of the data point. Grey colours indicate either negative  $\Delta_{18}$  or  $\Delta^{13}CH_3D$  values or sub-freezing temperatures. Circled samples have  $C_1/C_{2-3}$  values greater than  $10^5$ . Data from Stolper *et al.* (2014a, 2015) and Douglas *et al.* (2016, 2017).

### Clumped-isotope temperatures and the Whiticar plot

Figure 9 displays samples with measured clumped-isotope compositions in the Whiticar plot. Gases of known origins (thermogenic, biogenic and mixed origins – given by the symbols) fall within or close to the respective fields outlined by this space. Setting aside samples with non-equilibrium clumped-isotope values, one visible pattern is that there is a general clustering of samples with colder clumped-isotope-based temperatures (blue fill colours) with lower  $\delta D$  and  $\delta^{13}C$  values in the biogenic field to moderate clumped-isotope-based temperatures (purple fill colours) in the mixed field and then the warmest clumped-isotope-based temperatures (red fill colours) in the thermogenic field with the highest  $\delta D$  and  $\delta^{13}C$  values. Consequently, the clumped-isotope temperatures fit with the general expectations of gas origins predicted by the Whiticar plot.

There are, however, a few noticeable exceptions. For example conventional oil-associated gases can be found within the biogenic field with low  $\delta D$

values (c. 300‰) and/or low  $\delta^{13}\text{C}$  values ( $< -60\text{‰}$ ). Significantly, these designations are not based on the clumped-isotope temperatures. The clumped-isotope temperatures (all  $> 100^\circ\text{C}$ ) support these thermogenic designations. This is an example that shows thermogenic gases can exist outside the thermogenic regions delineated by the Whiticar plot and that clumped-isotope temperatures can provide the necessary fidelity to interpret these gases as thermogenic.

Figure 9 shows a clear separation of equilibrium v. non-equilibrium biogenic gases based on  $\delta\text{D}$  values, but not based on  $\delta^{13}\text{C}$  values – note that these figures only show measurements of environmentally derived samples and our discussion here is confined to such samples. Specifically, most biogenic gases with  $\delta\text{D}$  values less than  $-300\text{‰}$  have non-equilibrium clumped-isotope temperatures. In contrast, biogenic gases with  $\delta\text{D}$  values greater than  $-280\text{‰}$  yield meaningful clumped-isotope formation temperatures.

This delineation probably occurs because the same biochemical reactions control both the  $\delta\text{D}$  and the clumped-isotope values of biogenic methane. Specifically, when methanogens grow slowly, they appear to form methane in both clumped-isotopic equilibrium and hydrogen-isotopic equilibrium with water (Stolper *et al.* 2015; Wang *et al.* 2015). Consequently, both the  $\delta\text{D}$  value of the environmental waters as well as the methane-water hydrogen-isotope equilibrium fractionation factor will influence the  $\delta\text{D}$  value of the resultant biogenic methane. Specifically, at room temperature (c.  $25^\circ\text{C}$ ), methane  $\delta\text{D}$  values are c.  $180\text{‰}$  lower than in water at isotopic equilibrium (Stolper *et al.* 2015). Most waters, except those at latitudes higher than  $60^\circ$ , have  $\delta\text{D}$  values greater than  $-100\text{‰}$  (Bowen & Revenaugh 2003). Consequently,  $\delta\text{D}$  values of methane formed in isotopic equilibrium (including clumped) are typically restricted in the environment to values greater than c.  $-300\text{‰}$  (Fig. 9). In contrast, the formation of biogenic methane out of clumped-isotopic equilibrium is caused by kinetic isotope effects that result in methane  $\delta\text{D}$  values that are lower than values for isotopic equilibrium between methane and water (Stolper *et al.* 2015; Wang *et al.* 2015; Douglas *et al.* 2016). As a result, non-equilibrium clumped-isotope compositions commonly have  $\delta\text{D}$  values less  $-300\text{‰}$ . Thus, the biogenic field of the Whiticar plot when combined with clumped-isotope temperatures reveals the thermodynamic conditions (equilibrium v. non-equilibrium) of microbial methanogenesis. We note that the only exception to the c.  $-300\text{‰}$  methane  $\delta\text{D}$  delineation for samples in and out of clumped-isotopic equilibrium is a sample from the Birchtree mine (Young *et al.* 2017), which appears to have formed in clumped-isotopic equilibrium, but has a  $\delta\text{D}$  of  $-343\text{‰}$ . However, this sample is from a mine in Canada with highly depleted fluid  $\delta\text{D}$  values of  $-122\text{‰}$ ; Bottomley *et al.* 1994). Such fluids probably result in the exceptionally low methane  $\delta\text{D}$  values for the reasons given above.

Finally, samples that are a mixture of biogenic and thermogenic gas span a large range of  $\delta\text{D}$  and  $\delta^{13}\text{C}$  values. The clumped-isotope temperatures help

differentiate these samples. For example, gases with mixed compositions and  $\delta D$  and  $\delta^{13}C$  values that fall in the thermogenic field yield colder temperatures (bluer colours) than the pure thermogenic gases with similar  $\delta D$  and  $\delta^{13}C$  values (Fig. 9). Thus, clumped-isotope temperatures appear to be a useful tool for identifying gases with mixed origins in combination with the Whiticar plot.

#### Clumped isotopes and the Bernard plot

Figure 10 places clumped-isotope temperatures into the framework of the Bernard plot using the same symbols and colour scheme as in Figure 9. Fewer data are available for this comparison because not all gases with measured clumped-isotope temperatures have measured  $C_1/C_{2-3}$  ratios. The overall location of samples with known origin (thermogenic, biogenic or mixed) is generally consistent with those predicted by the Bernard plot.

As discussed previously, it has been suggested that thermogenic and biogenic gases can sit outside of the boundaries given by the Bernard plot (e.g. Martini *et al.* 1996; Vinson *et al.* 2017) – and this is supported by data with measured clumped-isotope values. For example,  $C_1/C_{2-3}$  values of non-associated unconventional gases can be greater than 100. Additionally, some conventional thermogenic gases lie outside of the thermogenic field. Specifically, these gases contain elevated  $C_2^+$  alkane contents ( $C_1/C_{2-3} < c.$  10) but also have  $\delta^{13}C$  values ( $-50$  to  $-64\text{‰}$ ), which are lower than ‘typical’ thermogenic gases. These gases have clumped-isotope temperatures that are consistent with their thermogenic origin ( $100$ – $135^\circ\text{C}$ ; purple-red colours in Fig. 10). This insight adds uncertainty to the common assumption that  $\delta^{13}C$  values less than  $-60\text{‰}$  positively identify biogenic methane (Bernard *et al.* 1976; Whiticar *et al.* 1986; Whiticar 1999), but supports models that predict methane formed at temperatures below *c.*  $180^\circ\text{C}$  can have low ( $< -60\text{‰}$ )  $\delta^{13}C$  values (Tang *et al.* 2000).

Finally biogenic gases generally have  $C_1/C_{2-3}$  values  $>100$ , as predicted by the Bernard plot. However, there are biogenic samples with  $C_1/C_{2-3}$  values as low as 43. These low  $C_1/C_{2-3}$  values may result from the presence of small amounts of thermogenic gas in these specific samples. However, the biogenic nature of these samples is supported by low ( $<50^\circ\text{C}$ ) clumped-isotope temperatures. Additionally, biogenic gases from sediments with far lower  $C_1/C_{2-3}$  values than 43 (as low as 2) have been described in which the ethane and propane are also thought to be biogenic in origin (Hinrichs *et al.* 2006). Thus the ethane in the examined samples is potentially biogenic. Consequently, the clumped-isotope temperatures may aid in interpreting whether a gas is an early formed thermogenic gas (clumped temperature  $>60^\circ\text{C}$ ), or a biogenic gas with a lower temperature regardless of the  $C_1/C_{2-3}$  ratio.

Values of  $\delta^{13}C$  and clumped-isotope temperatures of thermogenic gases



Here, we compare thermogenic methane  $\delta^{13}\text{C}$  values to clumped-isotope temperatures. We focus on methane  $\delta^{13}\text{C}$  values over  $\delta\text{D}$  values as the relationship between methane  $\delta^{13}\text{C}$  values to gas generation kinetics is better understood than for  $\delta\text{D}$  values, both from an observational and theoretical standpoint. The  $\delta^{13}\text{C}$  value of thermogenic methane is thought to be controlled by both the  $\delta^{13}\text{C}$  value of the source organic carbon and the thermal maturity at which the methane was generated. The relationship between  $\delta^{13}\text{C}$  and source maturity is generally explained by two mechanisms. First, it is assumed that elevated source-rock thermal maturities are achieved via exposure to higher burial temperatures or longer time spent at a given temperature (e.g. Burnham & Sweeney 1989; Sweeney & Burnham 1990). The kinetic isotope effects that describe the relative differences in the rate of methyl cleavage for  $^{12}\text{C}$  or  $^{13}\text{C}$  methyl groups have been modelled to decrease in magnitude with increasing temperature (Cramer *et al.* 1998; Tang *et al.* 2000; Xiao 2001). As methane is lower in  $\delta^{13}\text{C}$  than the source organic carbon (exhibiting a 'normal' isotope effect), higher temperatures result in methane with higher  $\delta^{13}\text{C}$  values relative to lower temperatures for a given methane source.

Second, the generation of methane, which has lower  $\delta^{13}\text{C}$  values than the source organic matter, due to mass balance considerations, will cause the residual organic carbon to increase in its  $\delta^{13}\text{C}$  value. This, in turn, causes newly generated methane to increase in  $\delta^{13}\text{C}$  values with increased hydrocarbon generation. Models describe this process using Rayleigh distillation frameworks of varying complexity (Clayton 1991; Berner *et al.* 1992, 1995; Cramer *et al.* 1998; Tang *et al.* 2000).

Ultimately, given the proposed dependence of methane's  $\delta^{13}\text{C}$  value on its source's thermal maturity, a positive relationship between methane  $\delta^{13}\text{C}$  values v. the clumped-isotope temperatures could be expected. We examine this idea using specific examples from Brazilian reservoirs and the full suite of data.

#### Specific examples from Brazilian reservoirs

A correlation between  $\delta^{13}\text{C}$  values and clumped-isotope temperatures of methane was first observed in Potiguar Basin samples (Brazil; conventional, oil-associated gases; Fig. 11a; Stolper *et al.* 2014a). This correlation was explained by the expected relationship between thermal maturity of the source rock and the  $\delta^{13}\text{C}$  value of the methane discussed above (Stolper *et al.* 2014a).

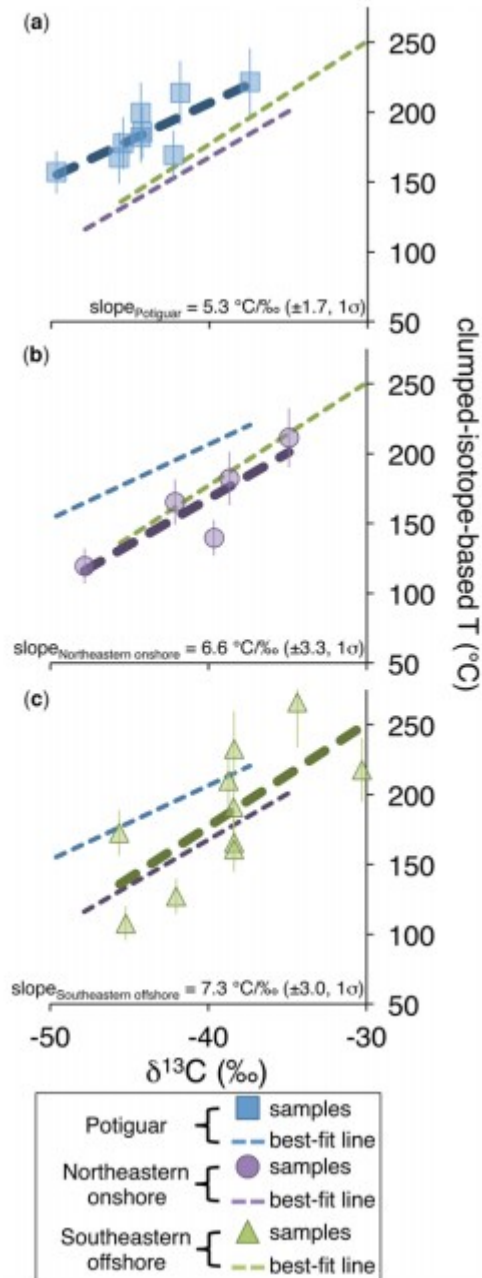


Fig. 11.

$\delta^{13}\text{C}$  values v. clumped-isotope-based temperatures from various Brazilian basins including (a) the Potiguar Basin, (b) the Northeastern Onshore Basin and (c) the Southeastern Offshore Basin. Dashed lines are best-fit lines. For clarity, regression lines are shown for other datasets when comparisons between data are made. In all cases a positive relationship between  $\delta^{13}\text{C}$  and the clumped-isotope-based temperature is observed. Data from Stolper *et al.* (2014a) and Douglas *et al.* (2017). Error bars are  $1\sigma$ .

We have observed correlations between methane  $\delta^{13}\text{C}$  values and clumped-isotope temperatures in two other conventional oil-associated systems in Brazil (referred to as the Northeastern Onshore Basin and Southeastern Offshore Basin; Douglas *et al.* 2017). The dependence of  $\delta^{13}\text{C}$  on formation

temperature for these three systems ranges from 5.3 to 7.3°C/‰, but all are within 1σ error of each other. Theoretical estimates for the change in δ<sup>13</sup>C of methane v. temperature solely due to temperature-dependent isotope effects for <sup>12</sup>C v. <sup>13</sup>C bond cleavage yield slopes from 8.8 to 9.4°C Ma<sup>-1</sup> (Tang *et al.* 2000; Ni *et al.* 2011; Stolper *et al.* 2014a). The lower slope measured for environmental samples compared to theory may result from the importance of distillation effects discussed above. Specifically, distillation increases the δ<sup>13</sup>C of methane as a function of thermal maturity in excess of that simply expected based on temperature-dependent kinetic isotope effects (which decreases the observed slope).

An interesting aspect of the clumped-isotope temperature v. δ<sup>13</sup>C relationships is that, although the slopes are all similar, the relationships are offset from each other. For example, the Potiguar Basin samples (Fig. 11a) v. the Northeastern Onshore Basin samples (Fig. 11b), at a given clumped-isotope temperature, differ by c. 6‰ in δ<sup>13</sup>C, with the Potiguar Basin sample being lower. This difference probably reflects a difference in the δ<sup>13</sup>C of the source organic carbon, which can vary among typically encountered source-rock compositions by c. 10‰ (e.g. Schoell 1984; Chung *et al.* 1992). As the clumped-isotope-based temperatures are not a function of the δ<sup>13</sup>C or δD of the source organic carbon, methane clumped isotopes can provide constraints on gas-formation temperatures (and source-rock thermal maturity) that do not require knowledge of the δ<sup>13</sup>C value of the source organic carbon.

#### General δ<sup>13</sup>C v. clumped-isotope trends

Thermogenic methane δ<sup>13</sup>C values v. clumped-isotope-based temperatures are compared in Figure 12 for all samples measured (as opposed to the Brazilian samples shown in Fig. 11). One general trend is that the δ<sup>13</sup>C and clumped-isotope temperatures of conventional oil-associated gases positively co-vary. There is significant scatter in this relationship that is not apparent when looking at specific gas accumulations (e.g. Fig. 11). This increased scatter is probably due to differences in the δ<sup>13</sup>C of the original source organic carbon of the different oil-associated reservoirs. For example, kerogen and oil δ<sup>13</sup>C values commonly vary from -32 to -22‰ (e.g. Schoell 1984; Chung *et al.* 1992).

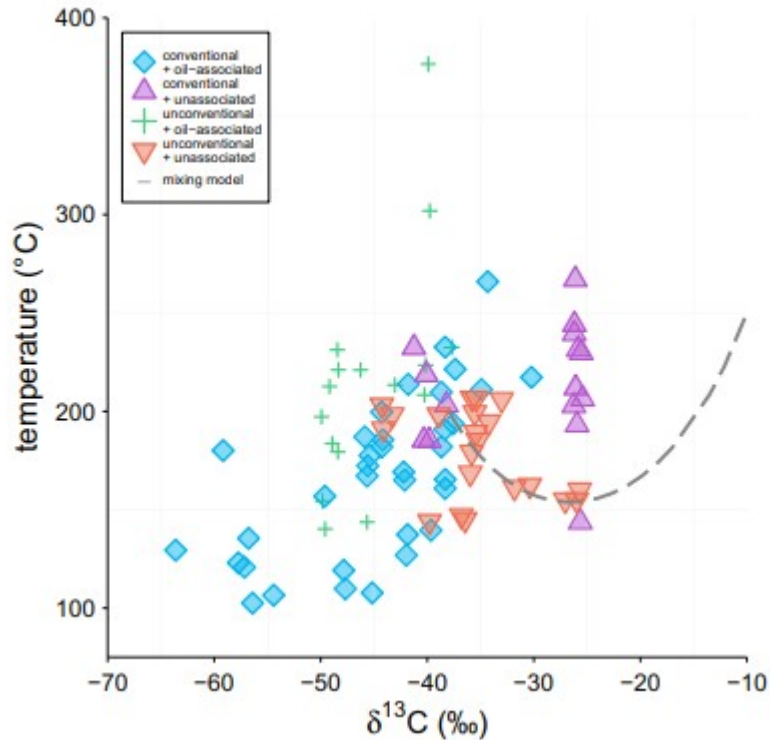


Fig. 12.

Comparison of  $\delta^{13}\text{C}$  values v. clumped-isotope temperatures from thermogenic gases. Data from Stolper *et al.* (2014a, b, 2015), Wang *et al.* (2015), Young *et al.* (2017) and Douglas *et al.* (2017). The modelled line shows the clumped-isotope-based temperature of a mixture of two end members. The first end-member gas has a  $\delta^{13}\text{C}$  of  $-38\text{‰}$ ,  $\delta\text{D}$  and  $-160\text{‰}$  and clumped-isotope temperature of  $200^\circ\text{C}$ , similar to the composition of numerous measured unconventional, non-associated gases. The second end member, a hypothetical high-maturity thermogenic gas, has a  $\delta^{13}\text{C}$  value of  $-10\text{‰}$  and  $\delta\text{D}$  value of  $-60\text{‰}$  (the approximate maximum values of thermogenic gases predicted by the models of Tang *et al.* (2000) and Ni *et al.* (2011)), and clumped-isotope formation temperature of  $250^\circ\text{C}$ . See text for details and discussion of the mixing line.

The conventional non-associated gases have generally higher  $\delta^{13}\text{C}$  values and clumped-isotope temperatures than conventional oil-associated gases. For  $\delta^{13}\text{C}$  values greater than  $-30\text{‰}$ , there is significant scatter of clumped-isotope temperatures. This comparison, though, is complicated by the fact that all of the conventional non-associated gases are derived fully or partially from coal sources. Coal-derived methane is known to have a different (and weaker)  $\delta^{13}\text{C}$  v. maturity relationship compared to other source-rock types (e.g. Type I and II kerogens; Schoell 1980).

The unconventional non-associated samples generally have elevated  $\delta^{13}\text{C}$  values and clumped-isotope temperatures compared to the conventional gases. Interestingly, these samples exhibit a different trend between  $\delta^{13}\text{C}$  and clumped-isotope-based temperature as compared to the oil-associated gases. For  $\delta^{13}\text{C}$  values less than  $-32\text{‰}$ , the conventional oil-associated gases and unconventional non-associated gases occupy a similar space (Fig. 12). However, all unconventional non-associated gases with  $\delta^{13}\text{C}$  values above  $-32\text{‰}$  yield clumped-isotope-based temperatures below  $165^\circ\text{C}$ . This

is the opposite of what would be expected based on the increasing trend defined by the conventional oil-associated gases. Furthermore, such elevated  $\delta^{13}\text{C}$  values are generally thought to be indicative of gas generation at temperatures above  $200^\circ\text{C}$  (Tang *et al.* 2000). We suggest that this apparent decline in clumped-isotope-based temperature as  $\delta^{13}\text{C}$  values increase above c.  $-32\text{‰}$  for unconventional non-associated gases is a result of mixing of gases produced at different maturities within the unconventional reservoir.

As discussed above, mixing of gases lower in  $\delta\text{D}$  and  $\delta^{13}\text{C}$  values with gases higher in  $\delta\text{D}$  and  $\delta^{13}\text{C}$  but identical  $\Delta_{18}$  values results in a mixture with a higher  $\Delta_{18}$  value (and thus lower clumped-isotope temperature) than either of the end members. Take, for example, the following mixing scenario between two end-member gases. Let the first end-member gas be a typical unconventional non-associated gas with a  $\delta^{13}\text{C}$  of  $-38\text{‰}$ ,  $\delta\text{D}$  of  $-160\text{‰}$  and clumped-isotope temperature of  $200^\circ\text{C}$  (Fig. 12.). Let the second end member be a high-maturity gas generated at  $250^\circ\text{C}$  with a  $\delta^{13}\text{C}$  value of  $-10\text{‰}$  and  $\delta\text{D}$  value of  $-60\text{‰}$  (the approximate maximum values of thermogenic gases predicted by the models of Tang *et al.* (2000) and Ni *et al.* (2011)). Mixing of this high-maturity gas into a larger reservoir of the typical nonconventional gas, due to the non-linear dependence of  $\Delta_{18}$  on the  $\delta^{13}\text{C}$  and  $\delta\text{D}$  values of mixtures, causes the clumped-isotope temperatures to initially decline. The trajectory of this mixing relationship is given in Figure 12. Only when the mixture is made up of 50% of this high-maturity gas do temperatures start increasing again.

Because modern models predict that methane formed at the end of hydrocarbon generation (i.e. the final c. 5% of total methane generated) can be significantly elevated in  $\delta\text{D}$  ( $>-60\text{‰}$ ) and  $\delta^{13}\text{C}$  ( $>-10\text{‰}$ ; Tang *et al.* 2000; Ni *et al.* 2011), we consider this conceptual model plausible to first order in explaining the lower clumped-isotope temperatures of the unconventional non-associated gases that have the highest  $\delta^{13}\text{C}$  values. Thus, production (and mixing) of a small amount of high maturity, high  $\delta^{13}\text{C}$  and  $\delta\text{D}$  gases into an unconventional gas reservoirs could conceivably lower the clumped-isotope based temperatures and explain the relationships observed between the clumped-isotope temperatures and methane  $\delta^{13}\text{C}$  values for non-associated, unconventional gases at the highest thermal maturities.

A synthesis of clumped-isotope studies and their utility in the study of economic accumulations of hydrocarbons

Here we examine a few simple scenarios that describe how methane clumped-isotope temperatures could be used to determine the origin of methane in naturally occurring hydrocarbon accumulations. Proper identification of the origin of methane accumulations could be used to constrain a model of the hydrocarbon system of interest by providing insight into gas generation and migration timing. Byrne *et al.* (2017) provide a more

general review of how geochemical techniques are used to study hydrocarbon systems.

### *Scenario 1: shallow microbial source*

Many microbial sources of methane are shallow in origin, generating methane within the first few hundreds of metres below the sediment–water interface. Because both a trap and seal are required to trap gas and because seals (other than methane hydrates) do not tend to develop sufficient capacity to hold hydrocarbons until sediments reach depths of c. 500 m (Rice & Claypool 1981), the generation of shallow microbial gas is unlikely to result in an economic gas accumulation. This situation is depicted as ‘Scenario 1’ in Figure 13 and Table 1. A gas of shallow microbial origin can be identified using its clumped-isotope composition in two ways. First, if the gas is generated slowly and is in clumped-isotope equilibrium, it will yield a low methane clumped-isotope temperature indicative of the shallow temperatures in the sediments (e.g. <25°C). Additionally, such a gas would be expected to be low in  $\delta^{13}\text{C}$  (e.g. <50‰), elevated in  $\delta\text{D}$  (> c. –300‰), and have a high  $\text{C}_1/\text{C}_{2-3}$  ratio (e.g. >100). Second, the gas could be generated out of clumped-isotope equilibrium. In such a case the clumped-isotope composition could be negative. However, non-equilibrium biogenic methane has been measured with apparent temperatures within the thermogenic gas range (e.g. c. 100–200°C; Wang *et al.* 2015; Douglas *et al.* 2016) and the origin of the gas could be incorrectly identified as thermogenic. Importantly, the  $\delta^{13}\text{C}$  of these gases is likely to be less than –50‰, the  $\delta\text{D}$  less than –300‰, and the  $\text{C}_1/\text{C}_{2-3}$  ratio greater than 100. A thermogenic gas with these characteristics is unlikely (Bernard *et al.* 1976; Whiticar 1999).

**Table 1.** *Origin, isotopic and compositional characteristics of gases*

Scenario	Source	In clumped-isotope equilibrium?	$\delta^{13}\text{C}$ (‰)	$\delta\text{D}$ (‰)	$\text{C}_1/\text{C}_{2-3}$ ratio	Clumped-isotope temperature (°C)
1	Shallow biological source	Yes	<–50	>–300	>100	<25
		No	<–50	<–300	>100	>100 and/or negative $\Delta_{18}$
2	Deep biological source	Yes	<–50	>–300	>100	c. 30–80
3	Thermogenic (oil-associated gas)	Yes (formed in oil window)	>–60	–	<10	60–160
		Yes (formed above oil window)	>–60	–	<10	>160
4	Thermogenic (non-associated gas)	Yes (formed in oil window)	>–60	–	>10	60–160
		Yes (formed above oil window)	>–60	–	>10	>160

These gases are discussed in the section ‘A synthesis of clumped-isotope studies and their utility in the study of economic accumulations of hydrocarbons’ and presented in Figure 13.

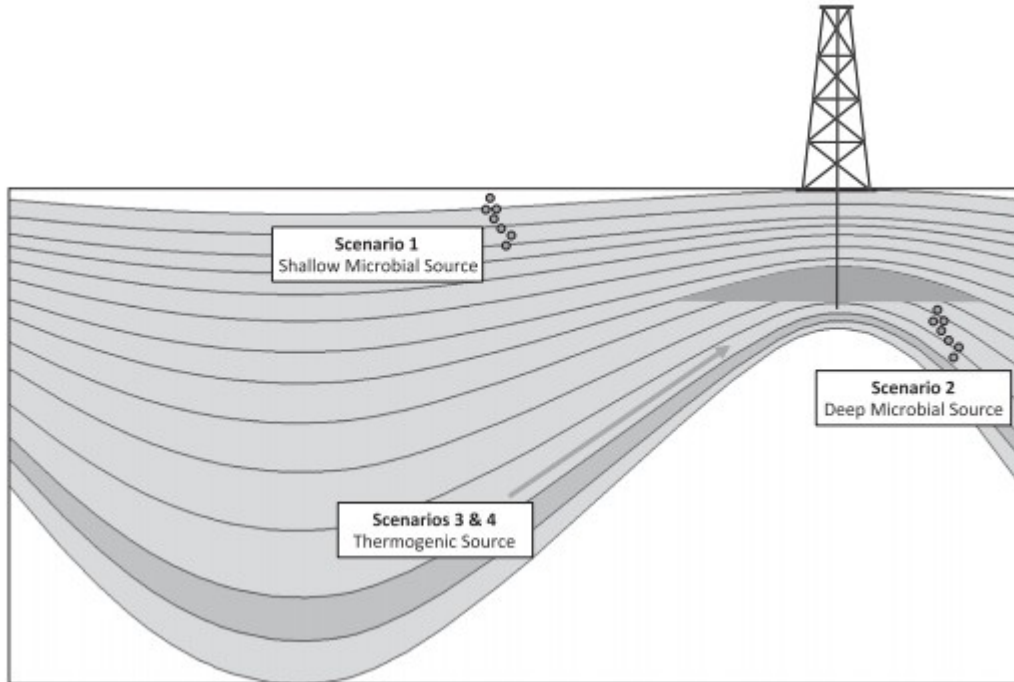


Fig. 13.

Conceptual figure of how methane clumped-isotope temperatures in combination with  $\delta D$  and  $\delta^{13}C$  values of methane and  $C_1/C_{2-3}$  values can be used to identify the source of natural gas in a sedimentary system as discussed in the section 'A synthesis of clumped-isotope studies and their utility in the study of economic accumulations of hydrocarbons'. Scenarios are given in both that section and Table 1. The arrow from Scenarios 3 and 4 represents migration of hydrocarbons to a reservoir rock (dark shaded area penetrated by the well).

#### *Scenario 2: deep microbial source*

Alternatively, microbial gases could be generated at sufficient depths (>500 m) to be trapped in the subsurface – such a situation is given by Scenario 2 in Figure 13 and Table 1. For this scenario, the clumped-isotope temperatures are expected to be between c. 30 to 80°C, with the upper limit derived from observations from nature (Wilhelms *et al.* 2001; Valentine 2011). These temperatures would correspond to maximum biogenic sources between 1500 and 3000 m (Valentine 2011). Such a gas may be distinguished from low maturity thermogenic gases generated at the onset of oil generation by having high (>100)  $C_1/C_{2-3}$  ratios.

#### *Scenarios 3 and 4: thermogenic gas*

The third and fourth scenarios describe gas with a thermogenic origin (Fig. 13 and Table 1). Scenario 3 is for an oil-associated gas, and scenario 4 is for a non-associated gas. Methane clumped-isotope temperatures for either scenario would be expected to be greater than c.60°C, and probably above 100°C. If the gas were oil-associated, it would probably be distinguished by having low  $C_1/C_{2-3}$  ratios (<10). This gas may also be associated with liquid hydrocarbon components (i.e. oil would be recovered with the gas). A non-associated gas would be expected to have elevated  $C_1/C_{2-3}$  ratios (e.g. >10).

In both scenarios (3 and 4) the methane would probably have  $\delta^{13}\text{C}$  values  $> -60\text{‰}$ . In either scenario, a key question is whether the gas formed with or without oil and whether after migration it became associated or non-associated. For example, an originally non-associated gas could become associated if it migrates to a reservoir that contains oil generated from a different source rock or at a different time than the gas. Alternatively, an originally oil-associated gas could become non-associated during migration during a phase separation. If the methane were formed with oil, the clumped-isotope temperatures should range from 60 to 160°C. If the methane formed at higher temperatures than oil generation, it would have higher temperatures ( $>160^\circ\text{C}$ ). This difference (formation with or without oil) dictates the generation and accumulation history of hydrocarbons in the basin. Such information could be used to constrain models of the basin's thermal history and the timing of hydrocarbon generation, migration and accumulation, and provides information on the original formation conditions of the gas.

In the scenarios given above, the sources were considered pure (i.e. the methane had one source). In the real world, traps can commonly contain mixtures of gases, both biogenic and thermogenic. Clumped isotopes are well suited to test for such mixtures and even enable the calculation of the contribution of the end members to the mixture. We explore one such example here. As discussed above, mixing of gases with the same clumped-isotope temperature but different  $\delta\text{D}$  and  $\delta^{13}\text{C}$  values such that one end member is lower in both, leads to a lowering of the clumped-isotope temperature as compared to linear mixing of  $\Delta_{18}$  values. The most extreme examples of such mixtures occur in systems in which a thermogenic gas with elevated  $\delta\text{D}$  and  $\delta^{13}\text{C}$  values mixes with a biogenic gas formed in or out of clumped-isotopic equilibrium, but with a low  $\delta^{13}\text{C}$  ( $< -60\text{‰}$ ) and low  $\delta\text{D}$  value ( $< -300\text{‰}$ ). In such cases, in the Arctic for example, clumped-isotope temperatures become exceptionally negative (as low as  $-60^\circ\text{C}$ ; Douglas *et al.* 2016). Such negative temperatures immediately imply that thermogenic gases exist in the system and are mixing with biogenic gases generated at shallow depths. Measurements of multiple gas samples in the area with different mixing ratios of these gases can be used to calculate the bulk and clumped-isotopic composition of the thermogenic end member and thus infer the temperature (and if a geotherm is known, the depth) at which the thermogenic component formed. An example of such a deconvolution is given in Douglas *et al.* (2016). Nonetheless, negative clumped-isotope temperatures, below the freezing point of water, are an immediate indication of the mixture of thermogenic and biogenic gases.

#### Questions moving forward

It is apparent that the clumped-isotope measurements of methane can provide new constraints on the conditions of methane generation. For biogenic gases formed slowly, thermogenic conventional oil-associated and non-associated gases, and unconventional non-associated gases, clumped-



isotope temperatures reflect the gas-formation temperatures. This allows clumped-isotope temperatures to be used to reconstruct the formational environments of the gases. Microbial gases generated rapidly are formed out of clumped-isotope equilibrium. This non-equilibrium signal can be used as a tracer of the rate of methanogenesis in the environment. We have outlined how these measurements can be placed in more typical gas interpretation frameworks that use the isotopic composition ( $\delta^{13}\text{C}$  and  $\delta\text{D}$ ) of methane and the molecular composition of the gas ( $\text{C}_1/\text{C}_{2-3}$  ratios) to constrain a sample's origins. The clumped-isotope compositions of methane often provide complementary and distinct information not contained in such frameworks. Finally, we have outlined a conceptual framework for how to interpret the meaning of clumped-isotope compositions in the context of gas exploration, highlighting how the clumped-isotope measurements provide unique constraints on the potential occurrence of hydrocarbon accumulations.

These examples indicate that methane clumped-isotope measurements are a promising tool for studying the generation and accumulation history of hydrocarbon deposits in nature. But many questions and future work exist and we outline a few here.

1. Why do oil-associated gases from unconventional reservoirs sometimes yield distinctly disequilibrium clumped-isotope compositions? Above we proposed that this may be the result of kinetic isotope effects associated with early stages of oil or bitumen cracking, or the means by which unconventional reservoirs are produced (via hydraulic fracking). This latter hypothesis could be tested by sampling gas from an oil-associated conventional reservoir over the course of its production history and examining if there are changes in both the bulk and clumped-isotopic composition. Nonetheless, more of these systems must be studied to understand why these systems are distinct from other thermogenic hydrocarbon accumulations.
2. Sophisticated models grounded in chemical kinetics exist to describe the formation of thermogenic oils and gases as a function of source organic type and thermal history. These models are routinely used to predict, based on an understanding of the geology of a system, where and when gas accumulations could have formed (Tissot & Welte 1978; Quigley & Mackenzie 1988; Burnham 1989; Behar *et al.* 1992, 1997; Pepper & Corvi 1995; Vandenbroucke *et al.* 1999; Tang *et al.* 2000; Lewan & Ruble 2002). Such models have been extended to include the evolution of  $\delta^{13}\text{C}$  and  $\delta\text{D}$  values of thermogenic gases (Tang *et al.* 2000; Ni *et al.* 2011). The addition of methane clumped-isotope constraints to such models is needed, but will require the effects of mixing to be considered. For example, extensive Rayleigh distillation of the source organic matter (which will result in methane with high  $\delta^{13}\text{C}$  and  $\delta\text{D}$  values) could create significant non-linear mixing effects for  $\Delta_{18}$  values.

3. How will independent  $^{12}\text{CH}_2\text{D}_2$  measurements contribute to the already measured  $\Delta_{18}$  and measurements discussed above? One aspect they will be able to test immediately is whether the interpretations put forward that many thermogenic and biogenic gases formed in isotopic equilibrium are correct. If the  $^{13}\text{CH}_3\text{D}$  and  $^{12}\text{CH}_2\text{D}_2$  values yield identical clumped-isotope temperatures, then this will provide strong support for the hypothesis that methane clumped-isotope temperatures can reflect thermogenic and biogenic gas-formation temperatures. Initial results of gases from pure-tank cylinders with  $\delta\text{D}$  and  $\delta^{13}\text{C}$  values consistent with a thermogenic origin as well as two natural gas samples, one from a Marcellus Shale deposit and one from a Utica Shale deposit, yield indistinguishable temperatures based on  $^{13}\text{CH}_3\text{D}$  and  $^{12}\text{CH}_2\text{D}_2$  values (Young *et al.* 2016) and thus provide initial support to this hypothesis. Additionally, biogenic gas from the Birchtree mine yields methane in clumped-isotope equilibrium for both  $^{13}\text{CH}_3\text{D}$  and  $^{12}\text{CH}_2\text{D}_2$  with temperatures (12–16°C) similar to the environmental temperatures (20–23°C), supporting the hypothesis that biogenic methane can form in clumped-isotopic equilibrium. Values of  $^{12}\text{CH}_2\text{D}_2$  will also play a useful role in distinguishing two-component mixing problems, as the non-linearity of mixing for  $^{12}\text{CH}_2\text{D}_2$  values depends solely on the  $\delta\text{D}$  value of the end member and not the  $\delta^{13}\text{C}$  values, which is not the case for  $^{13}\text{CH}_3\text{D}$ . The utility and power of these measurements will be realized in the near future as more measurements are made (Young *et al.* 2017). The frameworks presented above will need to incorporate these results.

4. Finally, other clumped and ‘position-specific’ isotopic measurements of hydrocarbons are beginning to be explored including  $^{13}\text{C}$ - $^{13}\text{C}$  ethane clumped-isotope measurements (Clog *et al.* 2014) and the propensity of  $^{13}\text{C}$  to be found on the exterior or interior carbon positions of propane (Gilbert *et al.* 2016; Piasecki *et al.* 2016). These measurements are reviewed in Eiler *et al.* (2017). As the information encoded by these measurements is understood new frameworks that incorporate the growing number of new isotopic measurements of hydrocarbons will need to be created.

#### Acknowledgements

This work was supported by the NSF, ExxonMobil, Petrobras, Statoil and Caltech. We thank ExxonMobil for permission to publish. This work was the outgrowth of a session at the 2015 Goldschmidt Conference. We wish to thank the other participants in the session for stimulating discussions of the work.

#### References

- Affek H.P. 2012. Clumped isotope paleothermometry: principles, applications, and challenges. *The Paleontological Society Papers*, 18, 101–114.
- Alexander R., Kagi R.I. & Larcher A.V. 1982. Clay catalysis of aromatic hydrogen-exchange reactions. *Geochimica et Cosmochimica Acta*, 46, 219–222.

Alexander R., Kagi R.I. & Larcher A.V. 1984. Clay catalysis of alkyl hydrogen exchange reactions - reaction mechanisms. *Organic Geochemistry*, 6, 755-760.

Ballentine C.J. & O'Nions R.K. 1994. The use of natural He, Ne and Ar isotopes to study hydrocarbon-related fluid provenance, migration and mass balance in sedimentary basins. *In: Parnell J. (ed.) Geofluids: Origin, Migration and Evolution of Fluids in Sedimentary Basins*. Geological Society, London, Special Publications, 78, 347-361,  
<https://doi.org/10.1144/GSL.SP.1994.078.01.23>

Behar F., Kressmann S., Rudkiewicz J. & Vandenbroucke M. 1992. Experimental simulation in a confined system and kinetic modelling of kerogen and oil cracking. *Organic Geochemistry*, 19, 173-189.

Behar F., Vandenbroucke M., Tang Y., Marquis F. & Espitalie J. 1997. Thermal cracking of kerogen in open and closed systems: determination of kinetic parameters and stoichiometric coefficients for oil and gas generation. *Organic Geochemistry*, 26, 321-339.

Bernard B.B., Brooks J.M. & Sackett W.M. 1976. Natural gas seepage in the Gulf of Mexico. *Earth and Planetary Science Letters*, 31, 48-54.

Bernard B.B., Brooks J.M. & Sackett W.M. 1977. A geochemical model for characterization of hydrocarbon gas sources in marine sediments. 9th Offshore Technology Conference Proceedings, Houston, TX, 3, 435-438.

Berner U., Faber E. & Stahl W. 1992. Mathematical simulation of the carbon isotopic fractionation between huminitic coals and related methane. *Chemical Geology*, 94, 315-319.

Berner U., Faber E., Scheeder G. & Panten D. 1995. Primary cracking of algal and landplant kerogens: kinetic models of isotope variations in methane, ethane and propane. *Chemical Geology*, 126, 233-245.

Bottomley D.J., Gregoire D.C. & Raven K.G. 1994. Saline ground waters and brines in the Canadian Shield: geochemical and isotopic evidence for a residual evaporite brine component. *Geochimica et Cosmochimica Acta*, 58, 1483-1498.

Bowen G.J. & Revenaugh J. 2003. Interpolating the isotopic composition of modern meteoric precipitation. *Water Resources Research*, 39, 9-1-9-13.

Burnham A. 1989. *A Simple Kinetic Model of Petroleum Formation and Cracking*. Lawrence Livermore National Lab, Report UCID 21665.

Burnham A.K. & Sweeney J.J. 1989. A chemical kinetic model of vitrinite maturation and reflectance. *Geochimica et Cosmochimica Acta*, 53, 2649-2657.

Burruss R. & Laughrey C. 2010. Carbon and hydrogen isotopic reversals in deep basin gas: evidence for limits to the stability of hydrocarbons. *Organic Geochemistry*, 41, 1285-1296.

Byrne D.J., Barry P.H., Lawson M. & Ballentine C.J. 2017. Noble gases in conventional and unconventional petroleum systems. *In*: Lawson M., Formolo M.J. & Eiler J.M. (eds) *From Source to Seep: Geochemical Applications in Hydrocarbon Systems*. Geological Society, London, Special Publications, 468. First published online December 14, 2017, <https://doi.org/10.1144/SP468.5>

Cao X. & Liu Y. 2012. Theoretical estimation of the equilibrium distribution of clumped isotopes in nature. *Geochimica et Cosmochimica Acta*, 77, 292–303.

Chung H., Gormly J. & Squires R. 1988. Origin of gaseous hydrocarbons in subsurface environments: theoretical considerations of carbon isotope distribution. *Chemical Geology*, 71, 97–104.

Chung H., Rooney M., Toon M. & Claypool G.E. 1992. Carbon isotope composition of marine crude oils (1). *AAPG Bulletin*, 76, 1000–1007.

Claypool G.E. & Kaplan I. 1974. The origin and distribution of methane in marine sediments. *In*:Kaplan I.R. (ed.) *Natural Gases in Marine Sediments*. Marine Science, 3, Springer, Boston, MA, 99–139.

Clayton C. 1991. Carbon isotope fractionation during natural gas generation from kerogen. *Marine and Petroleum Geology*, 8, 232–240.

Clog M., Martini A., Lawson M. & Eiler J. 2014. Doubly <sup>13</sup>C-substituted ethane in shale gases. Paper presented at the Goldschmidt Conference, Sacramento, CA, 435.

Clog M., Ellam R., Hilker A., Schwieters J. & Hamilton D. 2015. New developments in high-resolution gas source isotope ratio mass spectrometers. Paper presented at the AGU Fall Meeting, San Francisco.

Cramer B., Krooss B.M. & Littke R. 1998. Modelling isotope fractionation during primary cracking of natural gas: a reaction kinetic approach. *Chemical Geology*, 149, 235–250.

Curtis J.B. 2002. Fractured shale-gas systems. *AAPG Bulletin*, 86, 1921–1938.

Dennis K.J. & Schrag D.P. 2010. Clumped isotope thermometry of carbonatites as an indicator of diagenetic alteration. *Geochimica et Cosmochimica Acta*, 74, 4110–4122.

Dominé F., Bounaceur R., Scacchi G., Marquaire P.-M., Dessort D., Pradier B. & Brevart O. 2002. Up to what temperature is petroleum stable? New insights from a 5200 free radical reactions model. *Organic Geochemistry*, 33, 1487–1499.

Douglas P., Stolper D. et al. 2016. Diverse origins of Arctic and Subarctic methane point source emissions identified with multiply-substituted isotopologues. *Geochimica et Cosmochimica Acta*, 188,163–188.

Douglas P., Stolper D. et al. 2017. Methane clumped isotopes: progress and potential for a new isotopic tracer. *Organic Geochemistry*, 113, 262–282, <https://doi.org/10.1016/j.orggeochem.2017.07.016>

- Eiler J.M. 2007. 'Clumped-isotope' geochemistry – The study of naturally-occurring, multiply-substituted isotopologues. *Earth and Planetary Science Letters*, 262, 309–327.
- Eiler J.M. 2013. The isotopic anatomies of molecules and minerals. *Annual Review of Earth and Planetary Sciences*, 41, 411–441.
- Eiler J.M. & Schauble E. 2004.  $^{18}\text{O}^{13}\text{C}^{16}\text{O}$  in Earth's atmosphere. *Geochimica et Cosmochimica Acta*, 68, 4767–4777.
- Eiler J.M., Clog M. et al. 2013. A high-resolution gas-source isotope ratio mass spectrometer. *International Journal of Mass Spectrometry*, 335, 45–56.
- Eiler J.M., Clog M., Lawson M., Lloyd M., Piasecki A., Ponton C. & Xie H. 2017. The isotopic structures of geological organic compounds. *In: Lawson M., Formolo M.J. & Eiler J.M. (eds) From Source to Seep: Geochemical Applications in Hydrocarbon Systems*. Geological Society, London, Special Publications, 468. First published online December 14, 2017, <https://doi.org/10.1144/SP468.4>
- Ellam R., Newton J., Hilkert A., Schwieters J. & Deerberg M. 2015. Initial results from the SUERC 253 ultra: a new high resolution isotope Ratio Mass Spectrometer for Isotopologue Analysis. *Goldschmidt Conference Abstracts*, Prague, CZ, 822.
- Espitalie J., Ungerer P., Irwin I. & Marquis F. 1988. Primary cracking of kerogens. Experimenting and modeling  $\text{C}_1$ ,  $\text{C}_2$ – $\text{C}_5$ ,  $\text{C}_6$ – $\text{C}_{15+}$  classes of hydrocarbons formed. *Organic Geochemistry*, 13, 893–899.
- Etiopie G. & Sherwood Lollar B. 2013. Abiotic methane on Earth. *Reviews of Geophysics*, 51, 276–299.
- Ghosh P., Adkins J. et al. 2006.  $^{13}\text{C}$ – $^{18}\text{O}$  bonds in carbonate minerals: a new kind of paleothermometer. *Geochimica et Cosmochimica Acta*, 70, 1439–1456.
- Gilbert A., Yamada K., Suda K., Ueno Y. & Yoshida N. 2016. Measurement of position-specific  $^{13}\text{C}$  isotopic composition of propane at the nanomole level. *Geochimica et Cosmochimica Acta*, 177, 205–216.
- Hammes U., Hamlin H.S. & Ewing T.E. 2011. Geologic analysis of the Upper Jurassic Haynesville Shale in east Texas and west Louisiana. *AAPG Bulletin*, 95, 1643–1666.
- Helgeson H.C., Richard L., McKenzie W.F., Norton D.L. & Schmitt A. 2009. A chemical and thermodynamic model of oil generation in hydrocarbon source rocks. *Geochimica et Cosmochimica Acta*, 73, 594–695.
- Hinrichs K.-U., Hayes J.M. et al. 2006. Biological formation of ethane and propane in the deep marine subsurface. *Proceedings of the National Academy of Sciences*, 103, 14 684–14 689.

Hoering T. 1984. Thermal reactions of kerogen with added water, heavy water and pure organic substances. *Organic Geochemistry*, 5, 267–278.

Horibe Y. & Craig H. 1995. D/H fractionation in the system methane-hydrogen-water. *Geochimica et Cosmochimica Acta*, 59, 5209–5217.

Horita J. 2001. Carbon isotope exchange in the system CO<sub>2</sub>-CH<sub>4</sub> at elevated temperatures. *Geochimica et Cosmochimica Acta*, 65, 1907–1919.

Hunt J.M. 1996. *Petroleum Geochemistry and Geology*. W.H. Freeman and Company, New York.

Inagaki F., Hinrichs K.-U. et al. 2015. Exploring deep microbial life in coal-bearing sediment down to 2.5 km below the ocean floor. *Science*, 349, 420–424.

Jarvie D.M., Hill R.J., Ruble T.E. & Pollastro R.M. 2007. Unconventional shale-gas systems: the Mississippian Barnett Shale of north-central Texas as one model for thermogenic shale-gas assessment. *AAPG Bulletin*, 91, 475–499.

Killops S.D. & Killops V.J. 2013. *Introduction to Organic Geochemistry*. Blackwell, Oxford.

Google Scholar

Lash G.G. & Engelder T. 2011. Thickness trends and sequence stratigraphy of the Middle Devonian Marcellus Formation, Appalachian Basin: implications for Acadian foreland basin evolution. *AAPG Bulletin*, 95, 61–103.

Lee D.S., Herman J.D., Elsworth D., Kim H.T. & Lee H.S. 2011. A critical evaluation of unconventional gas recovery from the Marcellus Shale, northeastern United States. *KSCCE Journal of Civil Engineering*, 15, 679–687.

Lewan M. 1997. Experiments on the role of water in petroleum formation. *Geochimica et Cosmochimica Acta*, 61, 3691–3723.

Lewan M. & Ruble T. 2002. Comparison of petroleum generation kinetics by isothermal hydrous and nonisothermal open-system pyrolysis. *Organic Geochemistry*, 33, 1457–1475.

Liu Q. & Liu Y. 2016. Clumped-isotope signatures at equilibrium of CH<sub>4</sub>, NH<sub>3</sub>, H<sub>2</sub>O, H<sub>2</sub>S and SO<sub>2</sub>. *Geochimica et Cosmochimica Acta*, 175, 252–270.

Lorant F., Prinzhofer A., Behar F. & Huc A.-Y. 1998. Carbon isotopic and molecular constraints on the formation and the expulsion of thermogenic hydrocarbon gases. *Chemical Geology*, 147, 249–264.

Ma Q., Wu S. & Tang Y. 2008. Formation and abundance of doubly-substituted methane isotopologues (<sup>13</sup>CH<sub>3</sub>D) in natural gas systems. *Geochimica et Cosmochimica Acta*, 72, 5446–5456.

Magoon L.B. & Dow W.G. 1994. *The Petroleum System: From Source to Trap*. American Association of Petroleum Geologists.

- Mango F.D. & Hightower J. 1997. The catalytic decomposition of petroleum into natural gas. *Geochimica et Cosmochimica Acta*, 61, 5347–5350.
- Mango F.D., Hightower J. & James A.T. 1994. Role of transition-metal catalysis in the formation of natural gas. *Nature*, 368, 536–538.
- Martini A.M., Budai J.M., Walter L.M. & Schoell M. 1996. Microbial generation of economic accumulations of methane within a shallow organic-rich shale. *Nature*, 383, 155–158.
- Martini A.M., Walter L.M., Budai J.M., Ku T.C.W., Kaiser C.J. & Schoell M. 1998. Genetic and temporal relations between formation waters and biogenic methane: upper Devonian Antrim Shale, Michigan Basin, USA. *Geochimica et Cosmochimica Acta*, 62, 1699–1720.
- Martini A.M., Walter L.M., Ku T.C., Budai J.M., McIntosh J.C. & Schoell M. 2003. Microbial production and modification of gases in sedimentary basins: a geochemical case study from a Devonian shale gas play, Michigan basin. *AAPG Bulletin*, 87, 1355–1375.
- McCann T. 1998. The Rotliegendes of the NE German Basin: background and prospectivity. *Petroleum Geoscience*, 4, 17–27, <https://doi.org/10.1144/petgeo.4.1.17>
- Meissner F.F. 1978. Petroleum geology of the Bakken formation Williston Basin, North Dakota and Montana. *Economic Geology of the Williston Basin Symposium*. Montana Geological Society, Billings, Montana, 207–227.
- Miller S.M., Wofsy S.C. et al. 2013. Anthropogenic emissions of methane in the United States. *Proceedings of the National Academy of Sciences*, 110, 20 018–20 022.
- Mullen J. 2010. Petrophysical characterization of the Eagle Ford Shale in south Texas. Paper presented at the Canadian Unconventional Resources and International Petroleum Conference, Society of Petroleum Engineers.
- Ni Y., Ma Q., Ellis G.S., Dai J., Katz B., Zhang S. & Tang Y. 2011. Fundamental studies on kinetic isotope effect (KIE) of hydrogen isotope fractionation in natural gas systems. *Geochimica et Cosmochimica Acta*, 75, 2696–2707.
- Ono S., Wang D.T., Gruen D.S., Sherwood Lollar B., Zahniser M.S., McManus B.J. & Nelson D.D. 2014. Measurement of a doubly substituted methane isotopologue,  $^{13}\text{CH}_3\text{D}$ , by tunable infrared laser direct absorption spectroscopy. *Analytical Chemistry*, 86, 6487–6494.
- Passey B. & Henkes G. 2012. Carbonate clumped isotope bond reordering and geospeedometry. *Earth and Planetary Science Letters*, 351–352, 223–236.
- Pepper A.S. & Corvi P.J. 1995. Simple kinetic models of petroleum formation. Part I: oil and gas generation from kerogen. *Marine and Petroleum Geology*, 12, 291–319.

Pepper A.S. & Dodd T.A. 1995. Simple kinetic models of petroleum formation. Part II: oil-gas cracking. *Marine and Petroleum Geology*, 12, 321–340.

Peters K.E., Walters C. & Moldowan J. 2005. *The Biomarker Guide: Volume II. Biomarkers and Isotopes in Petroleum Systems and Earth History*. Cambridge University Press, Cambridge, UK.

Piasecki A., Sessions A., Lawson M., Ferreira A., Santos Neto E.V. & Eiler J.M. 2016. Analysis of the site-specific carbon isotope composition of propane by gas source isotope ratio mass spectrometer. *Geochimica et Cosmochimica Acta*, 188, 58–72.

Prinzhofer A.A. & Huc A.Y. 1995. Genetic and post-genetic molecular and isotopic fractionations in natural gases. *Chemical Geology*, 126, 281–290.

Quigley T. & MacKenzie A. 1988. The temperatures of oil and gas formation in the sub-surface. *Nature*, 333, 549–552.

Ranaweera H. 1990. *Sleipner Vest*. Graham & Trotman, London.

Reeves E.P., Seewald J.S. & Sylva S.P. 2012. Hydrogen isotope exchange between n-alkanes and water under hydrothermal conditions. *Geochimica et Cosmochimica Acta*, 77, 582–599.

Rice D.D. & Claypool G.E. 1981. Generation, accumulation, and resource potential of biogenic gas. *AAPG Bulletin*, 65, 5–25.

Rooney M.A., Claypool G.E. & Moses Chung H. 1995. Modeling thermogenic gas generation using carbon isotope ratios of natural gas hydrocarbons. *Chemical Geology*, 126, 219–232.

Sackett W.M. 1978. Carbon and hydrogen isotope effects during the thermocatalytic production of hydrocarbons in laboratory simulation experiments. *Geochimica et Cosmochimica Acta*, 42, 571–580.

Schoell M. 1980. The hydrogen and carbon isotopic composition of methane from natural gases of various origins. *Geochimica et Cosmochimica Acta*, 44, 649–661.

Schoell M. 1983. Genetic characterization of natural gases. *AAPG Bulletin*, 67, 2225–2238.

Schoell M. 1984. Recent advances in petroleum isotope geochemistry. *Organic Geochemistry*, 6, 645–663.

Seewald J.S. 2003. Organic–inorganic interactions in petroleum-producing sedimentary basins. *Nature*, 426, 327–333.

Seewald J.S., Benitez-Nelson B.C. & Whelan J.K. 1998. Laboratory and theoretical constraints on the generation and composition of natural gas. *Geochimica et Cosmochimica Acta*, 62, 1599–1617.

Shuai Y., Douglas P.M.J. et al. in press. Equilibrium and non-equilibrium controls on the abundances of clumped isotopologues of methane during



thermogenic formation in laboratory experiments: implications for the chemistry of pyrolysis and the origins of natural gases. *Geochimica et Cosmochimica Acta*.

Singh G. & Wolfsberg M. 1975. The calculation of isotopic partition function ratios by a perturbation theory technique. *The Journal of Chemical Physics*, 62, 4165–4180.

Stahl W.J. & Carey B.D. 1975. Source-rock identification by isotope analyses of natural gases from fields in the Val Verde and Delaware basins, west Texas. *Chemical Geology*, 16, 257–267.

Stolper D.A. & Eiler J.M. 2015. The kinetics of solid-state isotope-exchange reactions for clumped isotopes: a study of inorganic calcites and apatites from natural and experimental samples. *American Journal of Science*, 315, 363–411.

Stolper D.A., Lawson M. et al. 2014a. Formation temperatures of thermogenic and biogenic methane. *Science*, 344, 1500–1503.

Stolper D.A., Sessions A.L. et al. 2014b. Combined  $^{13}\text{C}$ -D and D-D clumping in methane: methods and preliminary results. *Geochimica et Cosmochimica Acta*, 126, 169–191.

Stolper D.A., Martini A.M. et al. 2015. Distinguishing and understanding thermogenic and biogenic sources of methane using multiply substituted isotopologues. *Geochimica et Cosmochimica Acta*, 161, 219–247.

Sweeney J.J. & Burnham A.K. 1990. Evaluation of a simple model of vitrinite reflectance based on chemical kinetics. *AAPG Bulletin*, 74, 1559–1570.

Takai K., Nakamura K. et al. 2008. Cell proliferation at 122°C and isotopically heavy  $\text{CH}_4$  production by a hyperthermophilic methanogen under high-pressure cultivation. *Proceedings of the National Academy of Sciences*, 105, 10 949–10 954.

Tang Y., Perry J., Jenden P. & Schoell M. 2000. Mathematical modeling of stable carbon isotope ratios in natural gases. *Geochimica et Cosmochimica Acta*, 64, 2673–2687.

Thauer R.K. 1998. Biochemistry of methanogenesis: a tribute to Marjory Stephenson. *Microbiology*, 144, 2377–2406.

Tissot B.P. & Welte D.H. 1978. *Petroleum Formation and Occurrence: A New Approach to Oil and Gas Exploration*. Springer-Verlag, Berlin.

Tsuzuki N., Takeda N., Suzuki M. & Yokoi K. 1999. The kinetic modeling of oil cracking by hydrothermal pyrolysis experiments. *International Journal of Coal Geology*, 39, 227–250.

Urey H.C. 1947. The thermodynamic properties of isotopic substances. *Journal of the Chemical Society*, 562–581.

- Valentine D.L. 2011. Emerging topics in marine methane biogeochemistry. *Annual Review of Marine Science*, 3, 147–171.
- Valentine D.L., Chidthaisong A., Rice A., Reeburgh W.S. & Tyler S.C. 2004. Carbon and hydrogen isotope fractionation by moderately thermophilic methanogens. *Geochimica et Cosmochimica Acta*, 68, 1571–1590.
- Vandenbroucke M., Behar F. & Rudkiewicz J. 1999. Kinetic modelling of petroleum formation and cracking: implications from the high pressure/high temperature Elgin Field (UK, North Sea). *Organic Geochemistry*, 30, 1105–1125.
- Vinson D.S., Blair N.E., Martini A.M., Larter S., Orem W.H. & McIntosh J.C. 2017. Microbial methane from in situ biodegradation of coal and shale: a review and reevaluation of hydrogen and carbon isotope signatures. *Chemical Geology*, 453, 128–145.
- Wang D.T., Gruen D.S. et al. 2015. Nonequilibrium clumped isotope signals in microbial methane. *Science*, 348, 428–431.
- Wang Z., Schauble E.A. & Eiler J.M. 2004. Equilibrium thermodynamics of multiply substituted isotopologues of molecular gases. *Geochimica et Cosmochimica Acta*, 68, 4779–4797.
- Webb M.A. & Miller T.F. III. 2014. Position-specific and clumped stable isotope studies: comparison of the Urey and path-integral approaches for carbon dioxide, nitrous oxide, methane, and propane. *The Journal of Physical Chemistry A*, 118, 467–474.
- Whiticar M.J. 1999. Carbon and hydrogen isotope systematics of bacterial formation and oxidation of methane. *Chemical Geology*, 161, 291–314.
- Whiticar M.J., Faber E. & Schoell M. 1986. Biogenic methane formation in marine and freshwater environments: CO<sub>2</sub> reduction vs acetate fermentation – isotope evidence. *Geochimica et Cosmochimica Acta*, 50, 693–709.
- Wilhelms A., Larter S., Head I., Farrimond P., Di-Primio R. & Zwach C. 2001. Biodegradation of oil in uplifted basins prevented by deep-burial sterilization. *Nature*, 411, 1034–1037.
- Wing B.A. & Halevy I. 2014. Intracellular metabolite levels shape sulfur isotope fractionation during microbial sulfate respiration. *Proceedings of the National Academy of Sciences*, 111, 18 116–18 125, <https://doi.org/10.1073/pnas.1407502111>
- Xia X. 2014. Kinetics of gaseous hydrocarbon generation with constraints of natural gas composition from the Barnett Shale. *Organic Geochemistry*, 74, 143–149.
- Xia X. & Tang Y. 2012. Isotope fractionation of methane during natural gas flow with coupled diffusion and adsorption/desorption. *Geochimica et Cosmochimica Acta*, 77, 489–503.

Xiao Y. 2001. Modeling the kinetics and mechanisms of petroleum and natural gas generation: a first principles approach. *Reviews in Mineralogy and Geochemistry*, 42, 383–436.

Young E.D., Rumble D., Freedman P. & Mills M. 2016. A large-radius high-mass-resolution multiple-collector isotope ratio mass spectrometer for analysis of rare isotopologues of O<sub>2</sub>, N<sub>2</sub>, CH<sub>4</sub> and other gases. *International Journal of Mass Spectrometry*, 401, 1–10.

Young E.D., Kohl I.E. et al. 2017. The relative abundances of resolved <sup>12</sup>CH<sub>2</sub>D<sub>2</sub> and <sup>13</sup>CH<sub>3</sub>D and mechanisms controlling isotopic bond ordering in abiotic and biotic methane gases. *Geochimica et Cosmochimica Acta*, 203, 235–264.